ERS-2

GOME Data Product Improvement Validation Report

Editor: B.Greco - ESA/ESRIN

Document ID: APP/AEF/17/BG
Issue: 1.0
Date: 31 August, 1998

European Space Agency
Agence spatiale européenne

ESRIN

Via Galileo Galilei - Casella Postale 64 - 00044 Frascati (Italy)
Tel. (39) 06 941801 - Fax (39) 06 94180 280

esa

ERS-2

Edited by: B. Greco

Contributing Authors:

D. Loyola
R. Spurr
B. Aberle
C. Bilinski
W. Thomas

A. Ladstätter-Weißenmayer
A. Richter
J.P. Burrows

J.C. Lambert
P.C. Simon

P. Stammes
R.B.A. Koelemeijer

Editor: B.Greco - ESA/ESRIN

Document ID: APP/AEF/17/BG
Issue: 1.0
Date: 31 August, 1998

TABLE OF CONTENTS

1 Introduction

After the initial validation phase, the distribution of GOME products started in August 1996. However, already at that time the validation team identified a number of highly desirable improvements to the products, and recommended to proceed to the implementation. Other recommendations came from individual users after the distribution of the early data.

DLR undertook the development work implementing the suggested changes in the new version of the GOME Data Processor. Different version numbers were then used for the different products, namely:

- Version 1.4 is the improved Level 1 product
- Version 2.3 is the improved Level 2 product

The product improvements have to be demonstrated with a validation exercise, with the following objectives:

- The verification of the changes correctness
- The assessment of the improvements of the geophysical parameters

The validation exercise is consequently focussed on the analysis of the differences with respect to the old version ad on their geophysical significance.

The exercise has been carried by different institutes, already familiar with the GOME data products, namely:

- DLR. Being also in charge of the development the report contains the list of software changes applied
- University of Bremen, focussing on the comparison with in-situ data for Ozone and Nitrogen Dioxide
- Belgian Institute for Space Aeronomy, focussing on the comparison with in-situ data for both Ozone and Nitrogen Dioxide
- Royal Dutch Meteorological Institute, focussing on polarisation correction and cloud detection

The following chapters are the reports by each contributing institute. The DLR report contains the description of the processing changes as well as the analysis of the product changes. The other chapters contain the report by the other institute, and are basically self-contained.

The validation dataset must represent as much as possible all observation conditions, but at the same time must be of small size, to limit the processing and analysis effort. This has led to the selection of a sparse dataset extending over the whole of year 1996 and beyond. Details are given in Chapter 1.

Internal Validation of GDP at DFD
Level 0-to-1 Version 1.4, Level 1-to-2 Version 2.3

D. Loyola, R. Spurr*, B. Aberle, C. Bilinski, W. Thomas

Deutsches Zentrum für Luft- und Raumfahrt (DLR)

Deutsches Fernerkundungsdatenzentrum (DFD)
Oberpfaffenhofen, D-82234 Weßling, Germany
(*) Harvard Smithsonian Center for Astrophysics, Cambridge, MA 02138, USA
E-mail: Diego.Loyola@dlr.de, http://auc.dfd.dlr.de/GOME

Internal Validation of GDP at DFD Level 0 to 1 Version 1.4, Level 1 to 2 Version 2.3

D. Loyola, R.Spurr, B. Aberle, C.Bilinski, W. Thomas

1. Introduction

This document describes recent changes to the GOME Data Processor with respect to the current operational version. First the changes in GDP in Level 0-to-1 and 1-to-2 are described, then results of the internal validation at DFD are shown, and finally some concluding remarks are given. The list of those validation orbits from 1996 and 1997 processed with the new version of GDP is attached in the appendix.

2. Changes in the GOME Data Processor

Changes in GDP 0-to-1 are classified in two parts: processor changes (changes that impact the binary level 1 product) and options in the extractor. Level 1-to-2 changes are classified by component algorithms.

2.1. GDP - Level 0-to-1 Processor

- Spatial aliasing correction using previous PMD for polarisation calculation
- Close geolocation gaps interpolating the scan mirror positions

2.2. GDP - Level 0-to-1 Extractor

- Calibration option "J", for radiance jump correction (available with version 1.3)
- Option '-r' to extract ground pixels between upper left and lower right corners
- Option '-n' to create one file without sun spectrum for each ground pixel
- Extraction software runs also on ALPHA computers and under the Linux operating system

2.3. GDP - Level 1-to-2

- ICFA: Use the correct slit function type
- DOAS: Use height of O_3 maximum number density instead of O_3 maximum VMR to determine Bass-Paur temperature
- AMF:
  - Use of parabolic weighting of AMFs
  - Three-month shift in the climatology readout corrected
  - Multiple scattering look-up table computed with GOMETRAN v. 2.0
  - New combined time/latitude interpolation scheme
  - Use of the USA climatology for NO_2

3. Internal Validation at DFD

3.1. GDP - Level 0-to-1 Processor

Internal validation of the GDP level 0-to-1 extractor (for example the radiance jumps correction) is not presented in this document, because the changes all involve options that do not affect the binary level 1 product (Note: the effect of jump corrections was discussed at the 5th GOME Working Session held at DLR, Oberpfaffenhofen, 18. February 1997).

- Spatial aliasing correction using previous PMD for polarisation calculation:
  The previous PMD readout is used for the determination and correction of polarisation. Figure 1(a) shows the effect of this change on the fraction of polarisation p for each of the three PMD detectors for a complete orbit. The polarisation correction factor is calculated with the following formula :

$$c_i = \frac{1}{2} \cdot \frac{1+\eta_i}{p_i \cdot (1-\eta_i) + \eta_i}$$

When spatial aliasing is switched on, the PMD values change and thus also the p values change at all wavelengths. Because eta and p are multiplied in above formula, the amplification of eta is different at each wavelength and so the structures of the eta function are expected to be obvious in the division of a spectrum with aliasing correction and a spectrum without aliasing correction. Figure 1(b) is an example of the effect of spatial aliasing change, the ratio is of the order of 0.2% with the shape of the eta function.

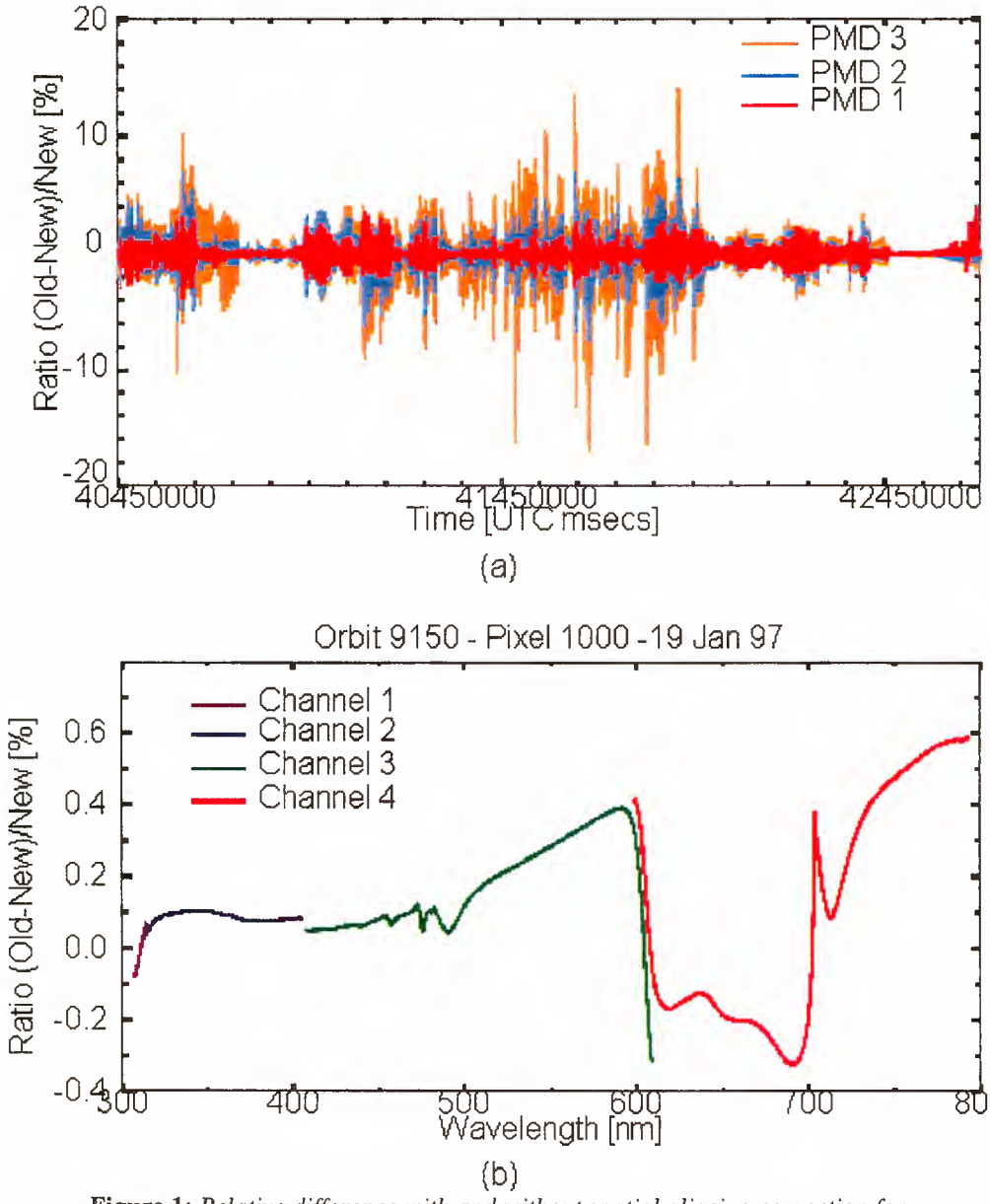

Figure 1: *Relative difference with and without spatial aliasing correction for (a) the fraction of polarisation p, and (b) Level 1 spectrum*

Close geolocation gaps interpolating the scan mirror positions.

The last scan mirror readout is extrapolated, allowing the gap to the first scan mirror readout of the next ground pixel to be closed. The effect on the ground pixel geolocation (a) before and (b) after the interpolation is shown in Figure 2.

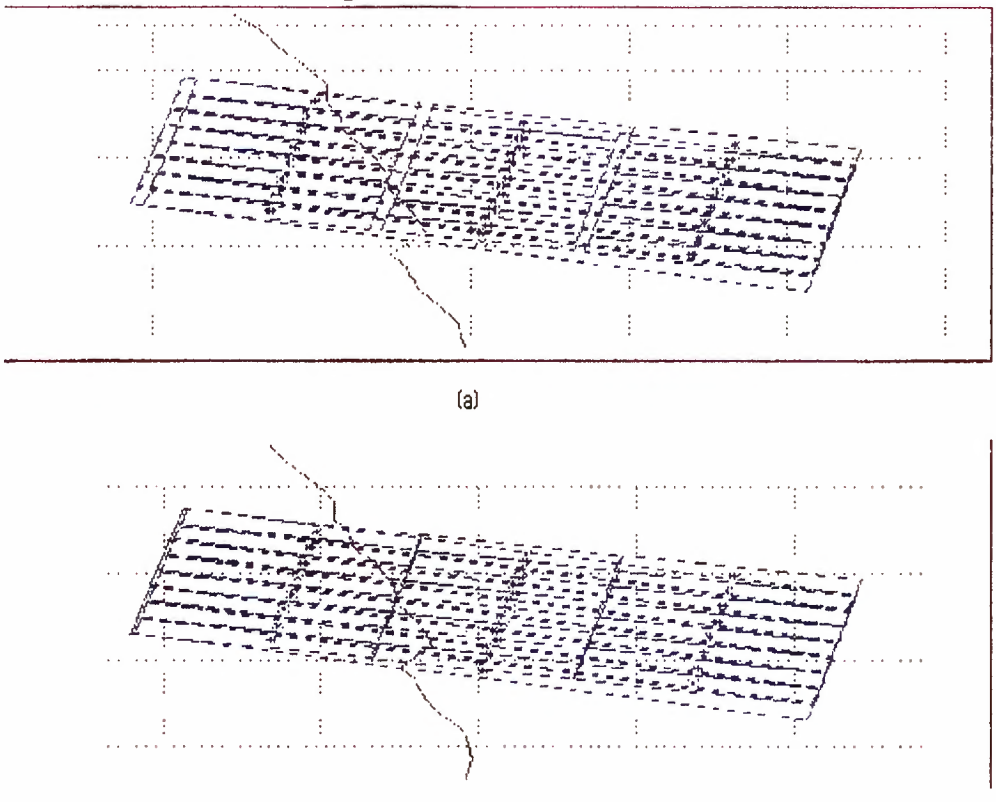

Figure 2: *Geolocation gaps (a) without and (b) with interpolation*

3.2. GDP - Level 1-to-2

Individual changes implemented on the ICFA, DOAS, and AMF component algorithms taken together in general produce compensating variations in the ozone vertical columns in most cases. For NO_2, there is a major change in the AMF due to the use of a different climatology. Four reference orbits (one for each season) have been selected to demonstrate the differences in the retrieved total columns of O_3 and NO_2 using the current operational version of GDP (2.0) and the new version (2.3). All results that follow are to be understood as ratios in retrieved trace gas column amounts between version (2.3) and version (2.0).

Generally, the implementation of the geometric (parabolic) weighting scheme for AMFs across the footprint field-of-view slightly decreases the final averaged AMF value, and hence the vertical column amount increases. For O_3, the use of that temperature where the maximum number density of O_3 occurs decreases the retrieved ozone vertical column amount by around 1.5%. For NO_2 major differences result from the use of the USA climatology; this has a sparser resolution in time and space but more reliable profile information in both winter hemispheres, The most obvious changes can be seen for the 'fall' and 'winter' scenarios, where the MPI NO_2 climatology has gaps (zero entries) in the concentration values for 'winter' in the high latitudes of both hemispheres.. The 3-month shift in the application of the MPI climatology is also a reason why the 'fall' scenarios are affected by changes in the NO_2 climatology. The computed AMFs for version (2.0) were too small and hence the NO_2 content was too high.

The spring scenario (orbit 5353, 28 Apr 1996, Figure 3) show an increase of O_3 in the northern hemisphere by about 4%, an increase in the tropics by about 1% and a decrease in the southern hemisphere by about 3% (mean values). The NO_2 content is lower in both hemispheres, by about 10% in

the northern midlatitudes and by about 5% in the southern midlatitudes. In the tropics, the NO_2 amount is relatively unchanged.

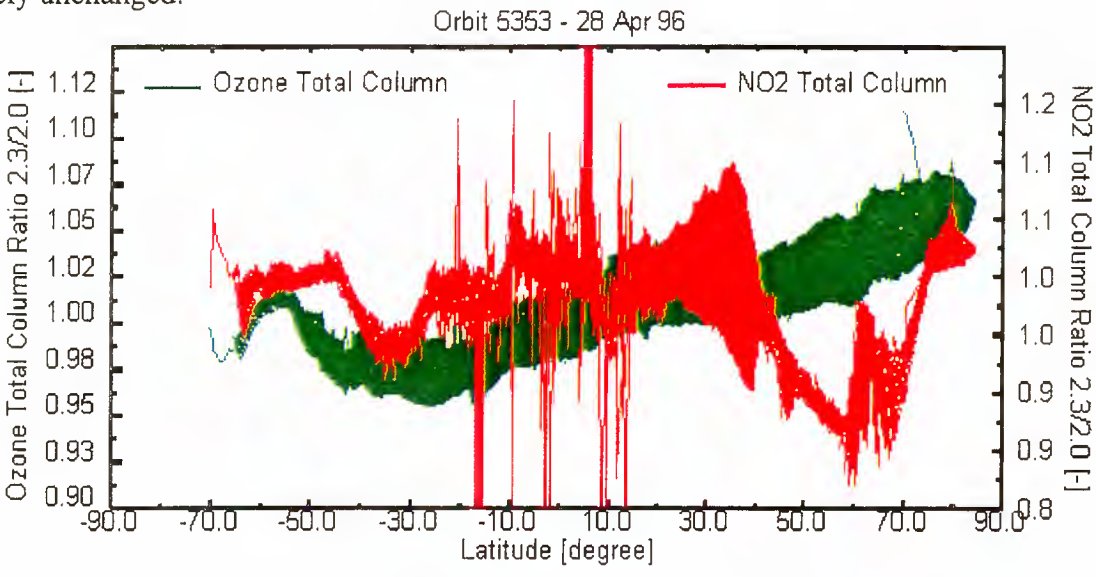

Figure 3: *Spring Scenario*

The summer scenario (orbit 6666, 29 Apr 1996, Figure 4) shows a general decrease towards the tropics where the ozone amount is now lower by about 4%. In both hemispheres, the ozone values are increased, by about 1% in the northern part and by about 2% in the southern hemisphere (where enhanced values are mainly observed in the midlatitude region). A similar behaviour is observed for the NO_2 AMFs but the changes are more pronounced. A decrease of about 50% is seen in the high northern latitude, with a decrease of around 10% in the southern midlatitudes (these changes are caused by the new AMF results). The tropical regions are only slightly affected and changes are around +/-10%; this may be due in part to unreliable climatology and a sensitivity to cloud fraction results.

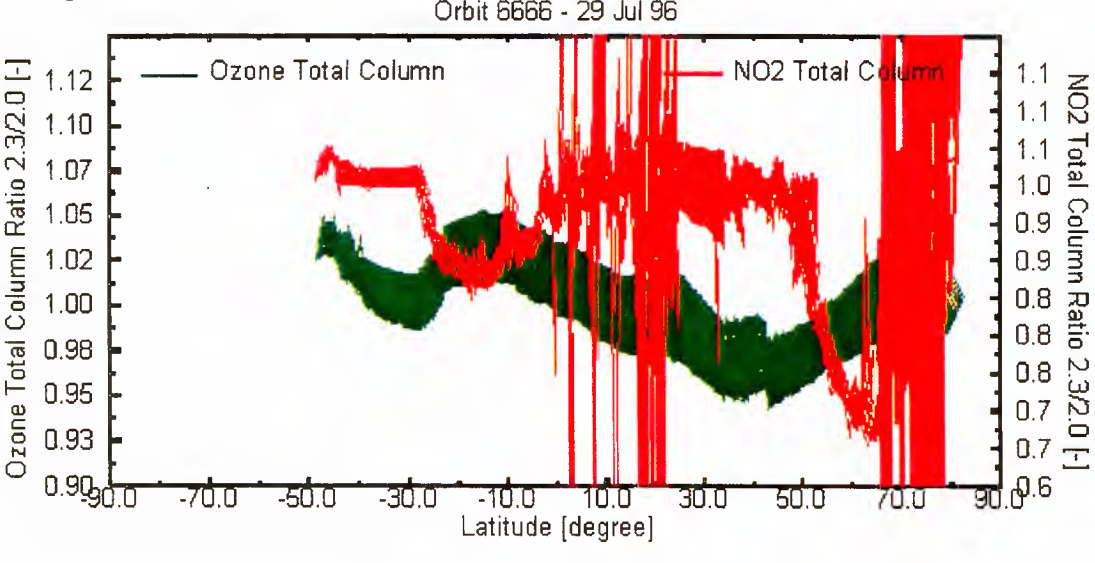

Figure 4: *Summer Scenario*

The fall scenario (orbit 7979, 29 Oct 1996, Figure 5) shows an orbit with partial coverage in the small footprint mode of GOME (40 x 40km). For this part of the orbit, variation across the entire footprint of each pixel is less pronounced (parabolic weighting has little effect on the average AMF). Generally, the ozone amount is enhanced in the high northern latitudes (2%) but decreases towards the tropics (5%) and increases slightly over the southern hemisphere (1%). A different behaviour is observed for NO_2 in

high northern latitudes (ca. 50% decrease), whereas NO_2 in the southern hemisphere is increased by around 5%.

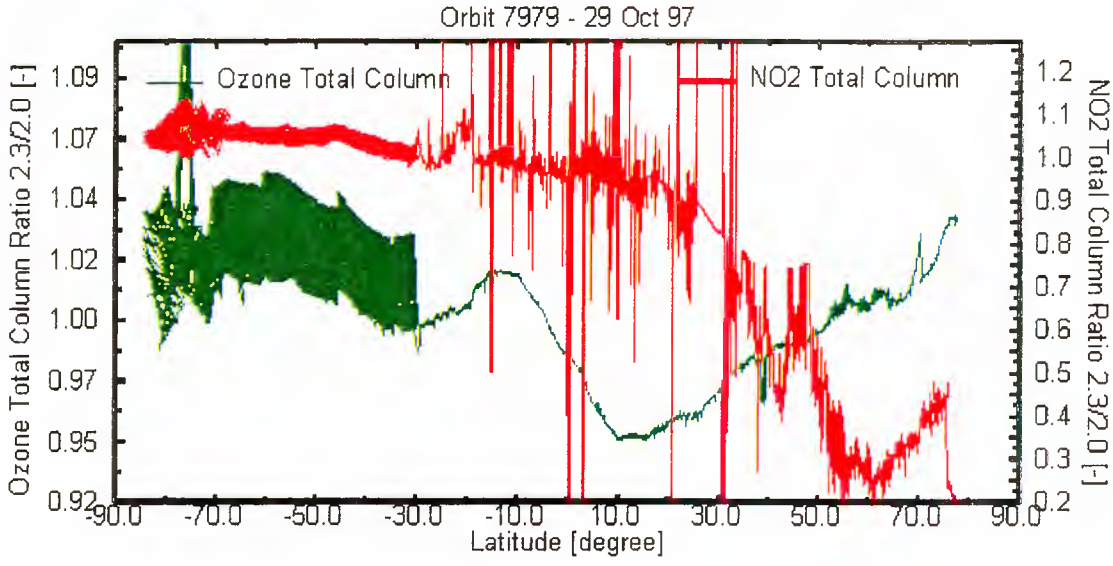

Figure 5: *Fall Scenario*

Finally, the winter scenario (orbit 9299, 29 Jan 1997, Figure 6) shows a slight increase in the O_3 content from northern latitudes towards the tropics (2.5%), followed by a decrease over the southern hemisphere of around 3%. A second increase in the O_3 amount is observed over the Antarctic subcontinent (1.5%). The NO_2 content is lower in the northern hemisphere by more than 50% at times, whereas the changes in the tropics are in the order of +/-5%.

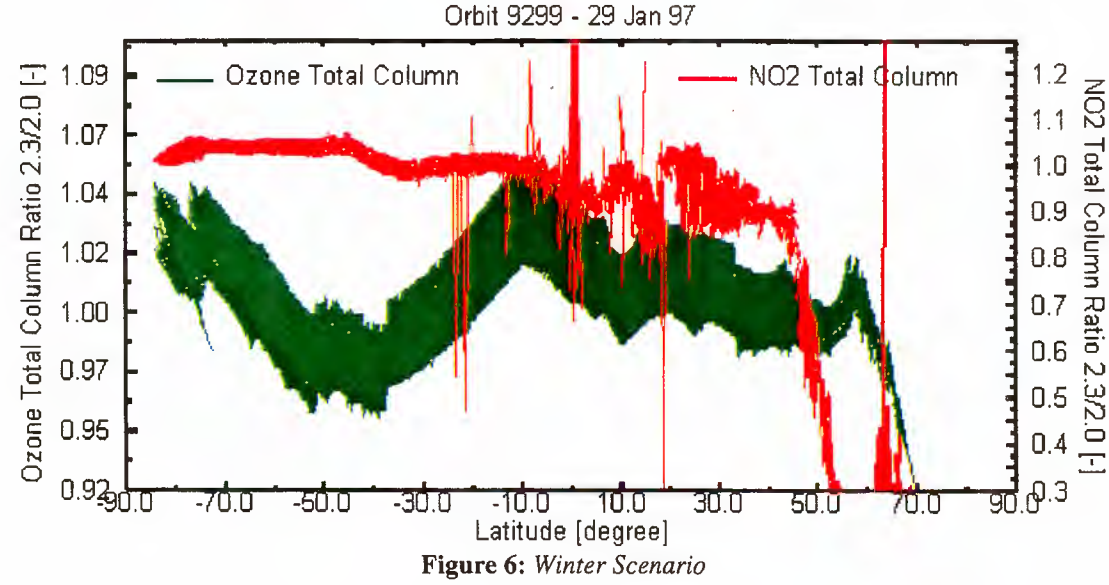

Figure 6: *Winter Scenario*

3.1.1. Effects of Single Algorithm Changes

A more detailed summary on the impact for ozone and NO_2 of each changed algorithms is given in table 1.

Table 1: Impact of Single Algorithm Changes

Module	Description	Impact on the level 2 product
ICFA	change of slit function type from 'rectangular' to 'simple hyperbolic'	total content O_3, NO_2 : approx. + 2%
DOAS	Use maximum ozone volume mixing ratio instead of maximum ozone number density to determine the Bass-Paur temperature	total content O_3 : approx. - 3% total content NO_2 : unchanged
AMF	Three months shift in trace gas climatology	total content O_3 : approx. ± 3% total content NO_2 : approx. ± 3% strongly seasonal dependent
AMF	AMF Look-up table calculated with three months shift in trace gas climatology	total content O_3 : approx. ± 2% total content NO_2 : approx. ± 2% strongly seasonal dependent
VCD	Parabolic weighting of AMF's across the footprint	total content O_3 : approx. + 2% total content NO_2 : approx. + 2% negligible for pixels with smaller swath (80 x 40 km^2)

3.2.1. East/Center/West/Backscan Differences

The trace gas content derived from the backscan pixel typically lied below the trace gas content derived from the three other pixel types. This was due to the fact that the final (representative) AMF was calculated as the average of AMFs computed at both edges and the centre of the pixel. Thus, the edges became too much weight and the averaged AMF was too high (! the trace gas vertical column was too low). Using a parabolic weighting scheme which gives the centre of any ground pixel the weight 4 and the edges the weight 1, the observed differences between the east, center, west and backscan ground pixel type are minimised (Figure 7). Now, the backscan pixel results is close to the results of the three other pixel types and even more, the backscan result can be seen as to be representative for the entire scan.

An additional weighting of AMFs is performed using simulated intensities, however, the intensity weighting scheme may not affect the ECWB- problem and is mentioned here just for completeness.

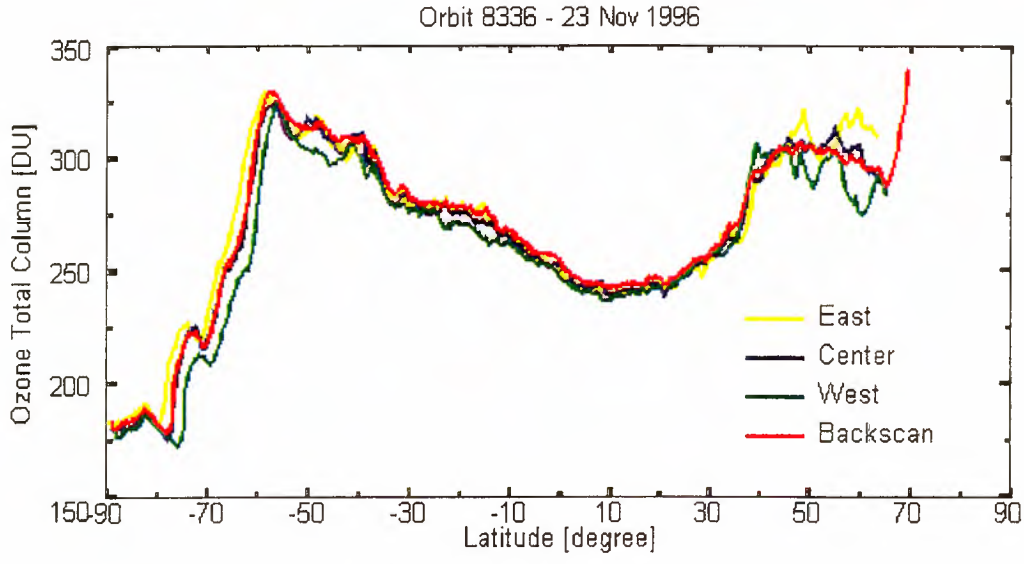

Figure 7: *ECWB Difference*

4. Conclusions

Changes to the Level 1 product are small, but polarization corrections are expected to be slightly improved, and the geolocation gaps are gone.

The variation on ozone total column is expected to be in the order of a few percent. The use of the USA climatology for NO_2 should produce more reliable values with a difference up to 50% in certain geographical regions with respect to the previous version.

Level 2 products for the polar view mode are included for the first time with the new version of GDP; this has become available after the computation of a complete set of AMF-MS correction factors for this viewing geometry. Results here should be treated with caution, as the used radiative transfer model is not wholly accurate for large line-of-sight zenith angles.

5. Postscript

Since October 1996, the GOME QA system at D-PAF has found some problems with the wavelength calibration. Lines at the beginning of channel 3 failed to meet the selection criteria and the wavelength calibration was wrong in a few cases.

The problems have arisen because of degradation in the GOME lamp. Version 1.35 of GDP Level 0-to-1, which has a weaker selection criteria for lines in channel 3, was put into operation. As a consequence, more spectral lines have been selected and the wavelength calibration in channel 3 has slightly changed.

The changes in wavelength and science data in channel 3 are slight, of the order of 1e-3. The effect on the NO_2 retrieved column amount is about 1% to 2%, though the precision of the fitting itself has shown a slight improvement.

In channel 2 where the UV ozone is retrieved, level 2 results are not affected by the updated version of GDP Level 0-to-1. The 1% differences in NO_2 are not significant compared with the expected 50% changes between the old and the new version of GDP Level 1-to-2.

Acknowledgements

The authors would like to thank the DLR-DFD colleague H. Mühle for his invaluable support during the selection and preparation of GOME validation data using the DMS system.

Appendix A

This appendix lists the orbits that were used for the validation acitivites.

The validation exercise involved Level-1 and Level-2 processing of almost 370 orbits, most of them from 1996. A set of consistent calibration parameters was also needed. To achieve this, the monthly calibration and the sun calibrations immediately before each validation orbit were processed with GDP Level 0-to-1 (additional 460 orbits).
Validation orbits from 1996 and 1997 are listed in the following tables.

Table 2: *Validation Orbits from January to June 1996*

	January 1996		Febr. 1996		March 1996		April 1996		May 1996		June 1996	
Day	Orbit	Start	Orbit	Start	Orbit	Start	Orbit	Start	Orbit	Start	Orbit	Start
1	3655	09:45:08	4105	20:14:36	4510	03:17:06	4960	13:46:30	5395	23:07:04		
2	3670	10:54:07	4120	21:23:35	4525	04:26:04	4975	14:55:29				
3	3685	12:03:05	4135	22:32:34	4540	05:35:03	4990	16:04:29	5410	00:16:03		
4	3701	14:52:40	4150	23:41:33	4555	06:44:02	5005	17:13:28	5425	01:25:02		
5	3715	14:21:03			4570	07:53:01	5020	18:22:27	5440	02:34:01	5886	06:21:01
6	3730	15:30:02	4165	00:50:32	4585	09:02:00	5035	19:31:26	5455	03:43:00	5905	14:12:24
7	3745	16:39:00	4180	01:59:31	4600	10:10:58	5050	20:40:26	5469	03:11:23	5920	15:21:23
8	3760	17:47:59	4195	03:08:30	4614	09:39:21	5065	21:49:25	5485	06:00:57	5935	16:30:22
9	3775	18:56:58	4210	04:17:29	4630	12:28:56			5500	07:09:56	5950	17:39:21
10	3790	20:05:57	4224	03:45:52	4645	13:37:54	5081	00:39:00	5515	08:18:55	5965	18:48:20
11	3805	21:14:55	4240	06:35:27			5095	00:07:23	5530	09:27:54	5980	19:57:19
12	3820	22:23:54	4255	07:44:26	4669 4676	05:52:16 17:36:28	5110	01:16:22	5545	10:36:53	5995	21:06:18
13	3835	23:32:53	4269	07:12:49	4691	18:45:26	5125	02:25:21	5560	11:45:52	6010	22:15:17
14			4285	10:02:24			5140	03:34:20	5575	12:54:50	6025	23:24:16
15	3850	00:41:51	4300	11:11:22	4720	19:22:48	5154	03:02:44	5590	14:03:49		
16	3866	03:31:25	4315	12:20:21	4735	20:31:46	5170	05:52:19	5605	15:12:48	6040	00:33:15
17	3881	04:40:25	4330	13:29:20	4750	21:40:45	5185	07:01:18	5620	16:21:47	6055	01:42:14
18	3895	04:08:48	4345	14:38:19					5635	17:30:46	6070	02:51:13
19	3917	17:01:59	4360	15:47:18	4780	23:58:42	5219	16:01:40	5650	18:39:45	6085	04:00:12
20			4375	16:56:17			5230	10:28:15	5665	19:48:44	6099	03:28:36
21			4390	18:05:16	4795	01:07:41	5245	11:37:14	5674	10:54:07	6115	06:18:11
22			4405	19:14:14	4811	03:57:15	5260	12:46:13			6130	07:27:10
23			4420	20:23:13	4825	03:25:37	5275	13:55:12	5710	23:15:40	6145	08:36:09
24			4435	21:32:12	4840	04:34:36	5290	15:04:11			6160	09:45:08
25			4450	22:41:11	4855	05:43:35	5305	16:13:10	5725	00:24:39	6175	10:54:07
26			4465	23:50:10	4870	06:52:35	5320	17:22:09	5740	01:33:37	6187 6197	07:01:18 23:47:17
27					4885	08:01:34	5335	18:31:08	5755	02:42:36	6205	13:12:04
28			4480	00:59:08	4900	09:10:33	5351	21:20:43	5770	03:51:35	6219	12:40:28
29			4495	02:08:07	4915	10:19:33	5365	20:49:06	5786	06:41:10	6235	15:30:02
30					4930	11:28:32	5381	23:38:41	5800	06:09:33	6250	16:39:01
31	4090	19:05:37			4945	12:37:31			5815	07:18:31		

Table 3: *Validation Orbits from July to December 1996*

	July 1996		August 1996		Sept. 1996		October 1996		Novem. 1996		Decem. 1996	
Day	Orbit	Start	Orbit	Start	Orbit	Start	Orbit	Start	Orbit	Start	Orbit	Start
1	6265	17:48:00	6700	03:08:27	7150 7156	13:37:53 23:41:29	7585	22:58:23	8020	08:18:52	8455	17:39:15
2	6280	18:56:59	6715	04:17:26	7165 7169	14:46:52 21:29:16			8035	09:27:51	8470	18:48:13
3	6295	20:05:58	6729	03:45:49	7178 7180	12:34:39 15:55:51	7600	00:07:21	8050	10:36:50	8485	19:57:10
4	6310	21:14:57	6745	06:35:23	7195	17:04:50	7615	01:16:20	8065	11:45:49	8500	21:06:10
5	6325	22:23:56	6760	07:44:22	7210	18:13:49	7630	02:25:19	8080	12:54:47	8515	22:15:09
6	6340	23:32:55	6775	08:53:21	7225	19:22:48	7645	03:34:18	8099	20:46:10	8530	23:24:08
7			6790	10:02:20	7240	20:31:47	7661	06:23:53	8110	15:12:45		
8	6355	00:41:54	6805	11:11:18	7255	21:40:46	7675 7685	05:52:15 22:38:15	8125	16:21:44	8545	00:33:07
9	6370 6371	01:50:53 03:31:29	6820	12:20:17	7269	21:09:09	7690	07:01:14	8132 8140	04:05:55 17:30:43	8560	01:42:06
10	6385 6389 6395	02:59:52 09:42:15 19:45:51	6835	13:29:16	7285	23:58:44	7705	08:10:13	8155	18:39:42	8583	16:15:53
11	6400	04:08:50	6850	14:38:14			7720	09:19:12	8170	19:48:40	8590	04:00:05
12	6414	03:37:13	6865	15:47:13	7300	01:07:43	7736	12:08:47	8185	20:57:39	8606	06:49:40
13	6430	06:26:48	6880	16:56:12	7315	02:16:42	7750	11:37:11	8200	22:06:38	8620	06:18:03
14	6445	07:35:47	6895	18:05:10	7330	03:25:41	7765	12:46:10	8214	21:35:01	8635	07:27:02
15	6460	08:44:46	6910	19:14:09	7345	04:34:40	7780	13:55:09			8650	08:36:01
16	6475	09:53:45	6925	20:23:08	7360	05:43:39	7795	15:04:08	8230	00:24:35	8665	09:45:00
17	6490	11:02:44	6940	21:32:06	7375 7384 7385	06:52:38 21:58:02 23:38:38	7810	16:13:07	8245	01:33:34	8680	10:53:59
18	6500 6505	03:48:43 12:11:42	6955	22:41:05	7390	08:01:37	7825	17:22:06	8260	02:42:33	8695	12:02:58
19	6520	13:20:41	6970	23:50:04	7405	09:10:36	7840	18:31:05	8275	03:51:31	8710	13:11:57
20	6535	14:29:40			7420	10:19:35	7855	19:40:04	8291	06:41:06	8725	14:20:56
21	6550	15:38:39	6985	00:59:02	7435	11:28:34	7870	20:49:03	8305	06:09:29	8740	15:29:55
22	6565	16:47:38	7000	02:08:02	7450	12:37:33	7885	21:58:02	8320	07:18:27	8755	16:38:54
23	6580	17:56:37	7015	03:17:01	7465	13:46:32			8335	08:27:26	8770	17:47:53
24	6589 6590 6595	09:02:00 10:42:36 19:05:36	7030	04:26:00	7480	14:55:31	7901	00:47:37	8350	09:36:25	8785	18:56:52
25	6610	20:14:34	7045	05:34:59	7495	16:04:29	7915 7929	00:16:00 23:44:23	8366	12:25:59	8800	20:05:51
26	6625	21:23:33	7060	06:43:58	7510	17:13:28	7930 7942	01:24:59 21:32:10	8380	11:54:22	8805 8809 8815	04:28:51 11:11:14 21:14:50
27	6640	22:32:32	7075	07:52:58	7525	18:22:27	7945	02:33:58	8395	13:03:20	8823 8825 8830	10:39:37 14:00:49 22:23:49
28	6655	23:41:31	7090 7091	09:01:57 10:42:33	7541	21:12:02	7960	03:42:56	8409	12:31:43		
29			7105	10:10:56	7555	20:40:25	7974	03:11:19	8425	15:21:17	8846	01:13:24
30	6670	00:50:29	7120	11:19:55	7570	21:49:24			8440	16:30:16		
31	6685	01:59:28	7135 7141	12:28:54 22:32:30			8012	18:54:05				

Table 4: *Validation Orbits from 1997*

Date	Orbit	Start
04-JAN-1997	8938	11:28:29
05-JAN-1997	8952	10:56:52
15-JAN-1997	9094	09:01:54
16-JAN-1997	9117	23:35:41
17-JAN-1997	9125	13:00:28
17-JAN-1997	9130	21:23:28
18-JAN-1997	9137	09:07:39
19-JAN-1997	9151	08:36:02
22-JAN-1997	9194	08:41:47
07-FEB-1997	9423	08:38:53
07-FEB-1997	9424	10:19:29
22-MAR-1997	10041	12:48:58
27-APR-1997	10556	12:17:20
29-APR-1997	10585	12:54:42

Investigation of GDP V2.0 and V2.3 O_3 and NO_2 measurements in Bremen and Ny-Ålesund

A. Ladstätter-Weißenmayer, A. Richter and J. P. Burrows

Institute of Environmental Physics, University of Bremen, Germany

Investigation of GDP V2.0 and V2.3 O_3 and NO_2 Measurements in Bremen and Ny-Ålesund

A. Ladstätter-Weißenmayer, A. Richter and J. P. Burrows

1. Introduction

In this report, the IUP-UB results from a comparison of GOME level-2 data using the current version 2.0 and an updated version 2.3 are summarised. Selected data sets of the 370 orbits provided by DLR have been compared of the GOME Data Processor (GDP) and the results analysed.
Two different exercises have been undertaken:

1. a direct comparison of the two versions of the GDP products, and
2. a validation using the ground-based measurements performed by the IUP Bremen in Bremen and Ny-Ålesund.

The results of the study are described below.

2. Comparison of GDP level 2 version 2.3 and 2.0 data

Nine orbits (see Annex 1) have been selected, and O_3 and NO_2 vertical columns from the level-2 product have been compared. To ensure the correct assignment of the individual pixels, only measurements, having the identical time in the data record, have been considered because other identification parameters, such as the naming scheme in the data record, were different in V2.0 and V2.3. This excludes the polar view data and a number of randomly distributed pixels, which are missing in either of the data sets for unknown reasons.
The relative changes for both O_3 and NO_2 are plotted as figures (see Annex1).

2.1. Investigation of ozone data

Most of the changes between V2.0 and V2.3 in ozone column are smaller than 5%. The only exceptions are measurements in the Arctic winter (Feb. 1996) and in September over Antarctica. For these pixels the new GDP version (V2.3) gives values, which are up to 10% smaller than those from the older and currently operational GDP(V2.0).
The differences show a clear dependence on latitude, with "edges" appearing at certain latitudes (0°, 10°, 30° - 40°, 60°; etc.) : values between these varying linearly. This probably results from changes in the AMF climatology and/or the corrected temperature for the ozone absorption cross-section.
One important point is the special behaviour of the back scan, which is clearly different from the other values in all the plots from April to December. For the back scan, there is a systematically larger change in values (5%) between the two versions. The sign of the change is often opposite to that for the other scan positions. The reason for this effect is the use of parabolic weighting of AMFs in the new GDP version. Measurements before March 1996 are not affected because of the smaller ground-pixels prior to the installation of the co-adding patch.

2.2. Investigation of NO_2

The changes in the NO_2 are much larger than those for O_3. This is particularly true in the Northern Hemisphere, where the changes are often 50% and more. There also is a large scatter in the relative

differences, which is mainly caused by small and noisy NO_2 columns near the equator. For those orbits having an error in the wavelength calibration between July and October 1997 in the operational data product, no useful comparison of the two data sets is possible.
In contrast to the O_3 data, no special behaviour of the back scan data is apparent. It has however to be noted, that such differences might be smaller than the scatter in the values and consequently not observed.

3. Validation of O_3 and NO_2 vertical columns using ground-based measurements

For the validation of the new level-2 products, all available GOME pixels within a 500 km radius of Bremen and Ny-Ålesund have been extracted and averaged. These values have then been compared to daily means (Ozone) or individual twilight measurements (NO_2) from the two ground-based instruments of the University of Bremen.
A summary of the dates for which data are available from both ground-based and GOME measurements is given in table 2 and 3 (see Annex 2).

3.1. O_3 data

The overall changes in O_3 are small (see above). Improvements with respect to the ground-based measurements are therefore expected to be small, and considering the measurement errors of 2-3% are relatively insignificant.

3.2. Bremen

In figure 1, the ozone values from GOME are compared with those from the IUP measurements. In figure 2, the relative differences (O_3 GOME - O_3 IUP) / O_3 IUP * 100 are given for both version 2.0 and 2.3 data. The general agreement is good with an average difference of -1.8% and a RMS of 4.5%. The numbers for the two versions of GOME data are summarised in table 4. For Bremen data no clear improvement in V2.3, with respect to V2.0 is obtained from this comparison.

3.3. Ny-Ålesund

O_3 values for Ny-Ålesund are given in fig. 3. The differences between ground-based and satellite data are larger than in Bremen (see fig.4 and table 4) and show no clear trend. The large difference present in the V2.0 of GOME are smaller in V2.3.

Table 4: Relative differences for Ozone between GOME and ground-based measurements

Location	Relative Difference [%]	Standard Deviation [%]
Bremen OLD	-1.8	4.4
Bremen NEW	-1.9	4.5
Ny-Ålesund OLD	-3.0	9.4
Ny-Ålesund NEW	-1.8	9.5

3.4. NO_2 data

Comparisons similar to those for O_3 were carried out for NO_2.

3.5. Bremen

In figure 5 the vertical column amounts for the GOME and ground-based data are shown for the trace gas NO_2 [molec/cm^2] at the location Bremen as function of day (day 1 is the 21st of April 1995). In this figure the morning and evening data were plotted for the ground-based measurements, and the „old" and „new" GOME-data: the GOME-data being the operational data products received from the DLR-DFD. In figure 6, the relative differences (NO_2 GOME - NO_2 IUP) / NO_2 IUP * 100 are given for both version 2.0 and 2.3 data.

3.6. Ny-Ålesund

Figure 7 shows the same comparison for the location Ny-Ålesund. In this case smaller differences were observed between the GOME and the ground-based data for both V2.0 and V2.3 GOME data than in Bremen. This is explained by the influence of tropospheric NO_2, which is much larger in Bremen than in Ny-Ålesund.
For both locations smaller differences relative to the ground-based measurements were observed when using in „new" GOME-data. The relative deviation (NO_2GOME - NO_2IUP)/NO_2 IUP * 100) is shown in the figures 6 and 8 for both locations.

For Bremen the maximum relative deviation was -700% for the „old" GOME-data and 300% for the „new" GOME-data for the trace gas NO_2. For the location Ny Alesund we observed a maximum deviation of 800% for the „old" GOME-data and 200% for the „new" GOME-data.

4. Summary

For Ozone, the changes between version 2.0 and version 2.3 data are relatively small (< 5% in most cases). Some Arctic and Antarctic measurements show larger differences. The observed changes are in the order of magnitude expected considering the changes in AMF climatology and ICFA.
No clear improvement of the GOME ozone values could be observed with respect to the ground-based measurements in Bremen and Ny-Ålesund. The general agreement remains good at the mid-latitude site of Bremen and relatively poor at Ny-Ålesund. While part of the differences seen result from the spatial and temporal variability of ozone, there still seem to be systematic errors in the GOME data.
For NO_2, the differences between the versions are much larger than for ozone. This is particularly true for the Northern Hemisphere, where the changes are often larger than 50%.
The general agreement with the ground-based measurements improved significantly, and is now often within a few percent. However, there still are many negative values for NO_2 in some orbits which is indicative of errors in either the data or the data processing.

5. Recommendations

- As a consequence of the results reported above, the University of Bremen recommends to update the GDP at DLR to version 2.3.

- For NO_2 at low latitudes averaging or smoothing of data needs to be invoked to reduce the noise in the signal.
- The implementation of "modified DOAS" for high latitudes in the next GDP version.
- The investigation and implementation of improved trace gas climatologies for the next GDP version.

6. Comments

During the validation exercise, some problems were encountered which unnecessarily complicated the work:

- changes in names of individual orbits.
- changes in pixel numbers.
- "random" gaps in some orbits.
- the use of those orbits with wavelength calibration errors in the operational data product makes these data useless for NO_2 validation.
- many compensating changes to the algorithm, which make it impossible to decide which of the changes in the new GDP version are responsible for improvements in the data, and therefore should be implemented. This is particularly true for NO_2.
  It is therefore advised that for future validation exercises naming schemes are maintained, where possible, or if they are changed then this is notified explicitly within the data set.

Annex: 1

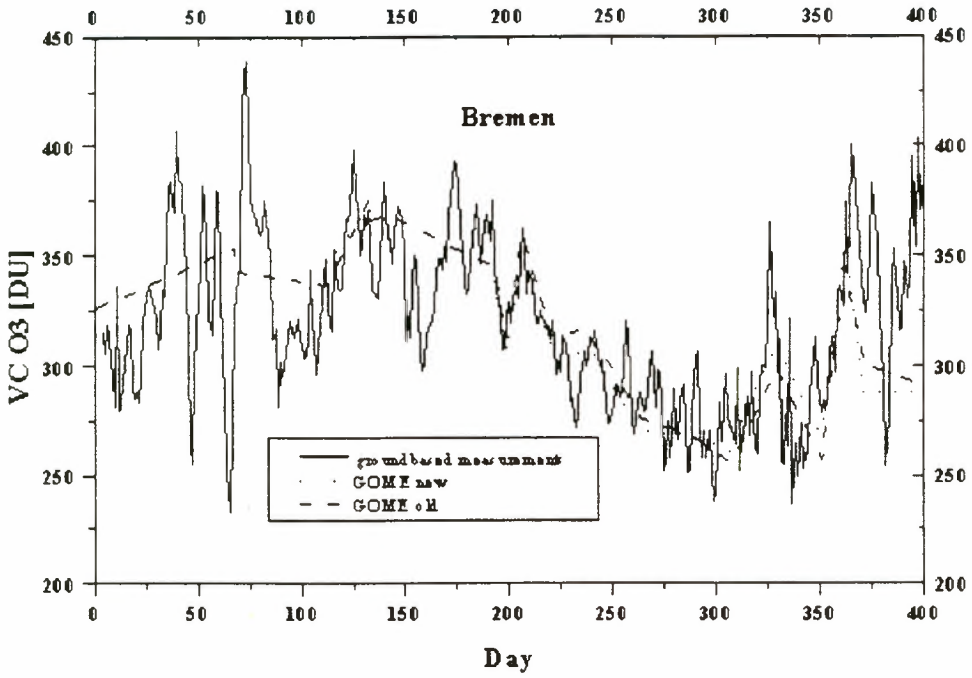

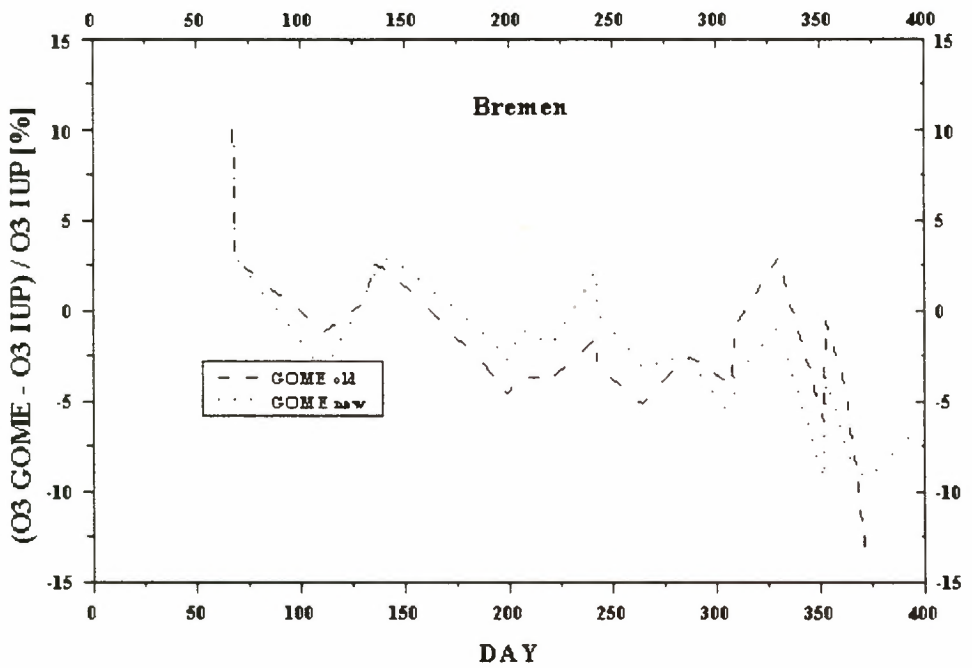

Figure. 1: *O_3 values from GOME are compared with those from the IUP measurements for Bremen.*
Figure. 2: *Relatives differences (O_3 GOME – O_3 IUP) / O_3 IUP)*100 are given for both version 2.0 and 2.3 data.*

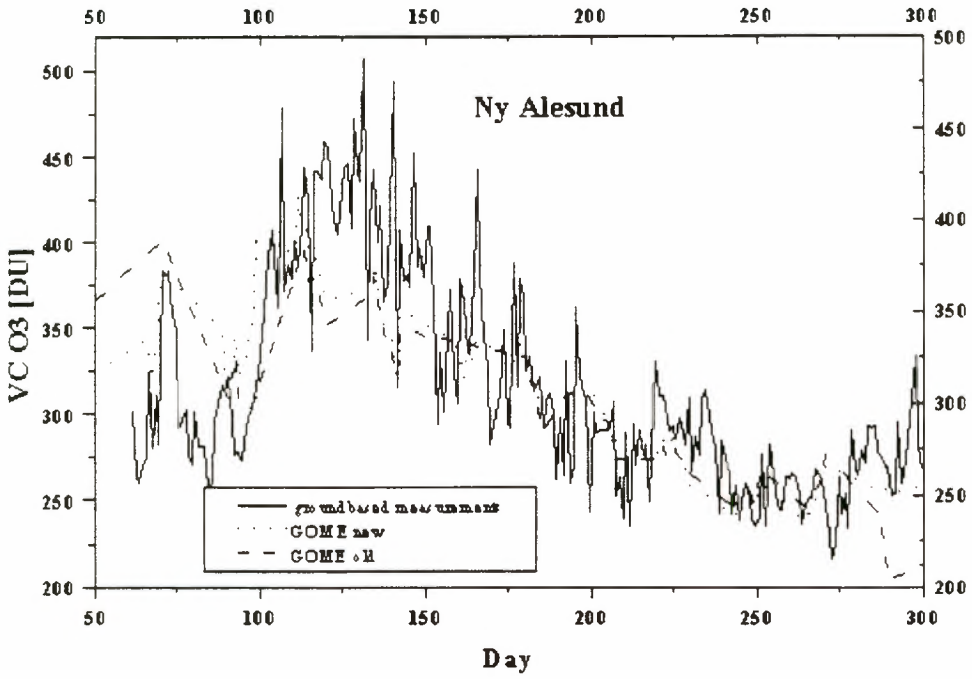

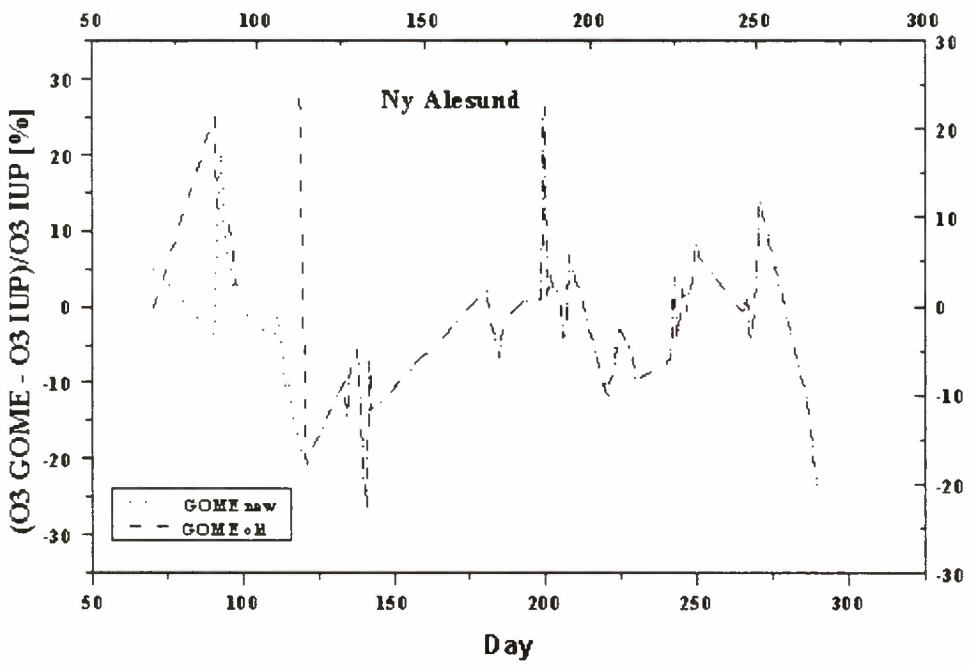

Figure. 3: *O_3 values from GOME are compared with those from the IUP measurements for Ny Alesund.*
Figure. 4: *Relatives differences (O_3 GOME – O_3 IUP) / O_3 IUP)*100 are given for both version 2.0 and 2.3 data.*

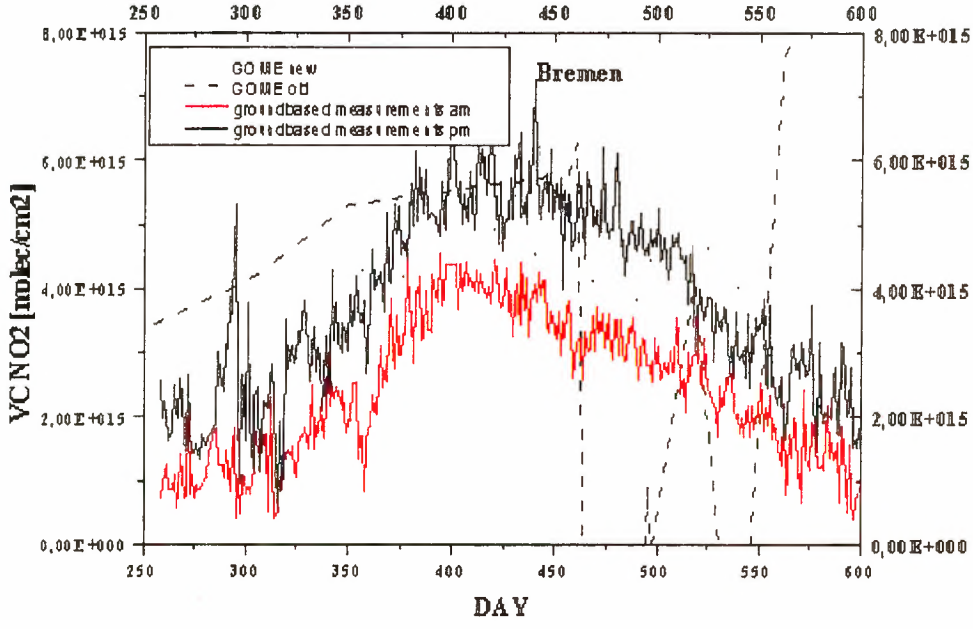

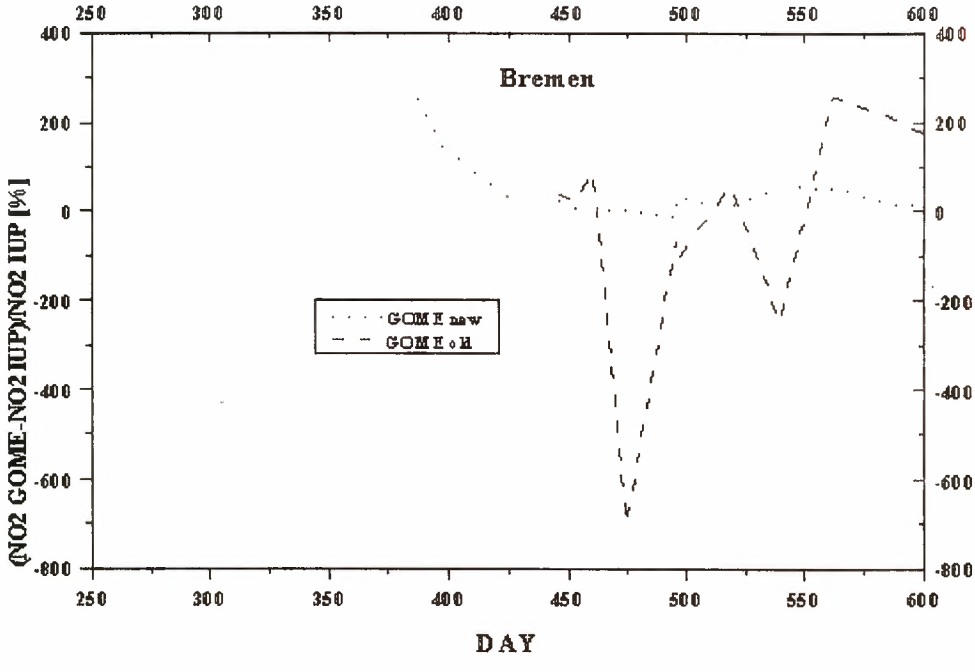

Figure. 5: *NO_2 values from GOME are compared with those from the IUP measurements for Bremen.*
Figure. 6: *Relatives differences (NO_2 GOME – NO_2 IUP) / NO_2 IUP)*100 are given for both version 2.0 and 2.3 data.*

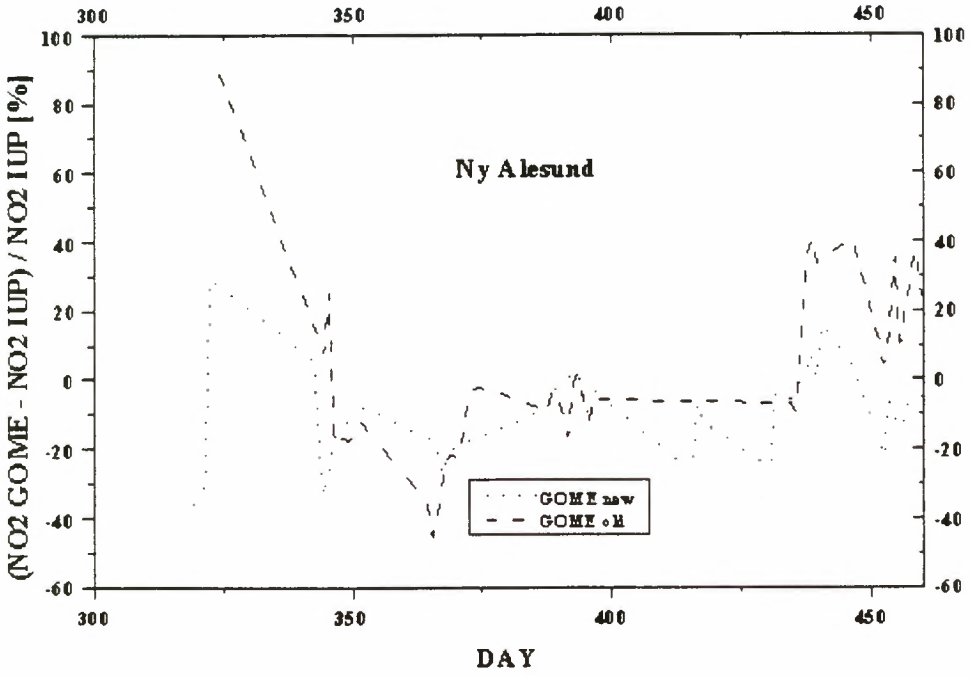

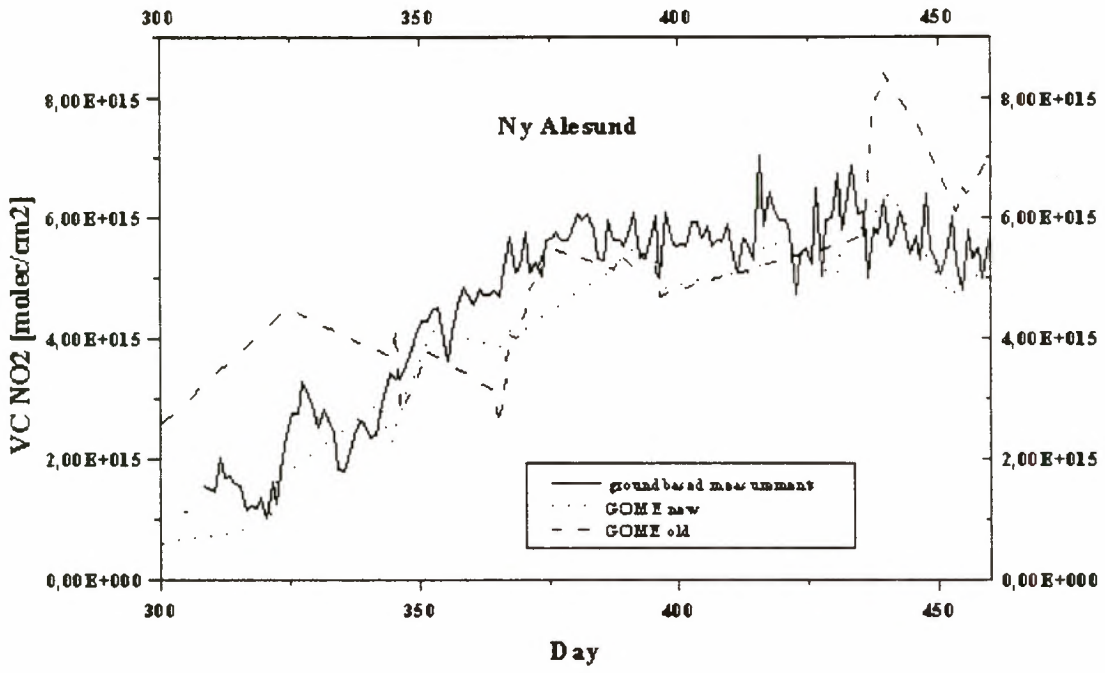

Figure. 7: *NO_2 values from GOME are compared with those from the IUP measurements for Ny Alesund.*
Figure. 8: *Relatives differences (NO_2 GOME – NO_2 IUP) / NO_2 IUP)*100 are given for both version 2.0 and 2.3 data.*

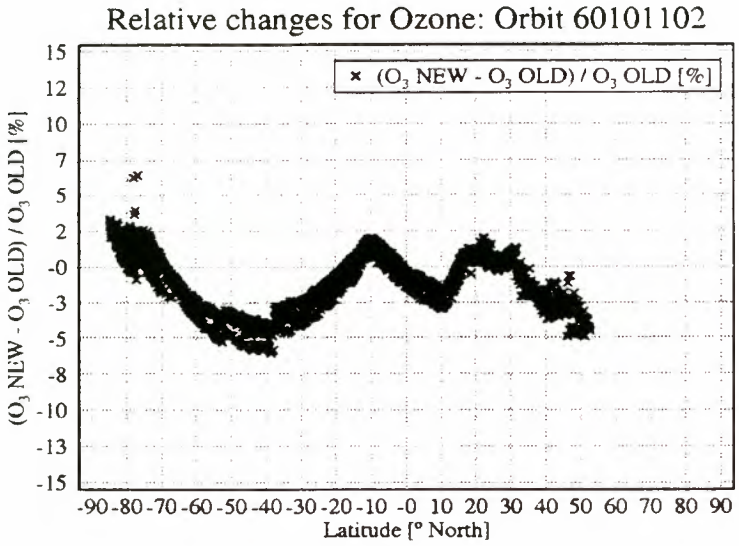
Relative changes for Ozone: Orbit 60101102
(O3 NEW - O3 OLD) / O3 OLD [%]
(O3 NEW - O3 OLD) / O3 OLD [%]
15 12 10 7 5 2 -0 -3 -5 -8 -10 -13 -15
-90 -80 -70 -60 -50 -40 -30 -20 -10 -0 10 20 30 40 50 60 70 80 90
Latitude [° North]

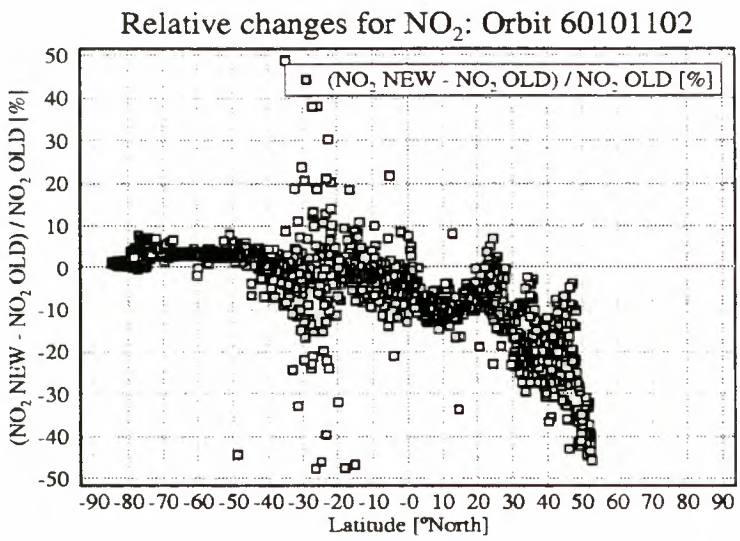
Relative changes for NO2: Orbit 60101102
(NO2 NEW - NO2 OLD) / NO2 OLD [%]
(NO2 NEW - NO2 OLD) / NO2 OLD [%]
50 40 30 20 10 0 -10 -20 -30 -40 -50
-90 -80 -70 -60 -50 -40 -30 -20 -10 -0 10 20 30 40 50 60 70 80 90
Latitude [°North]

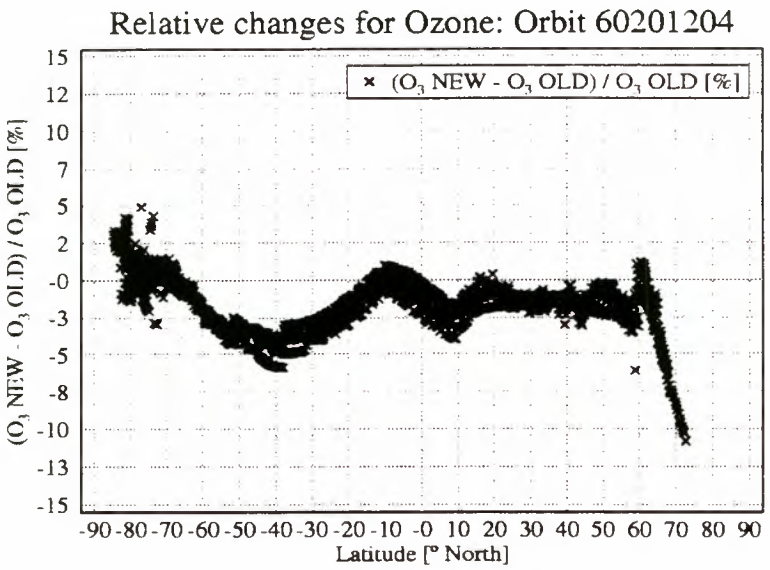
Relative changes for Ozone: Orbit 60201204
(O3 NEW - O3 OLD) / O3 OLD [%]
(O3 NEW - O3 OLD) / O3 OLD [%]
15 12 10 7 5 2 -0 -3 -5 -8 -10 -13 -15
-90 -80 -70 -60 -50 -40 -30 -20 -10 -0 10 20 30 40 50 60 70 80 90
Latitude [° North]

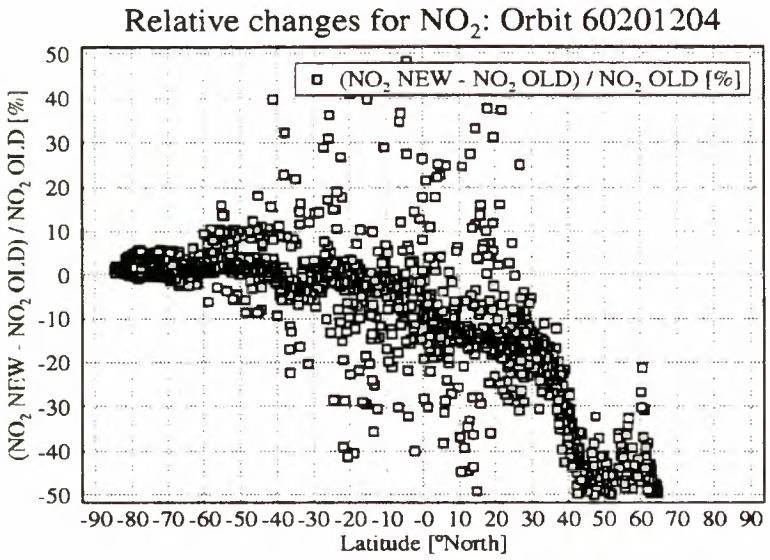
Relative changes for NO2: Orbit 60201204
(NO2 NEW - NO2 OLD) / NO2 OLD [%]
(NO2 NEW - NO2 OLD) / NO2 OLD [%]
50 40 30 20 10 0 -10 -20 -30 -40 -50
-90 -80 -70 -60 -50 -40 -30 -20 -10 -0 10 20 30 40 50 60 70 80 90
Latitude [°North]

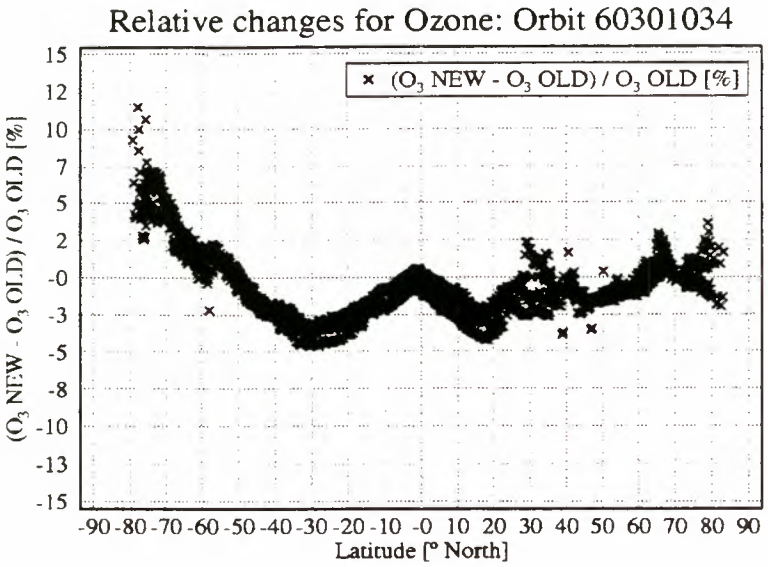
Relative changes for Ozone: Orbit 60301034
(O3 NEW - O3 OLD) / O3 OLD [%]
(O3 NEW - O3 OLD) / O3 OLD [%]
15
12
10
7
5
2
-0
-3
-5
-8
-10
-13
-15
-90 -80 -70 -60 -50 -40 -30 -20 -10 -0 10 20 30 40 50 60 70 80 90
Latitude [° North]

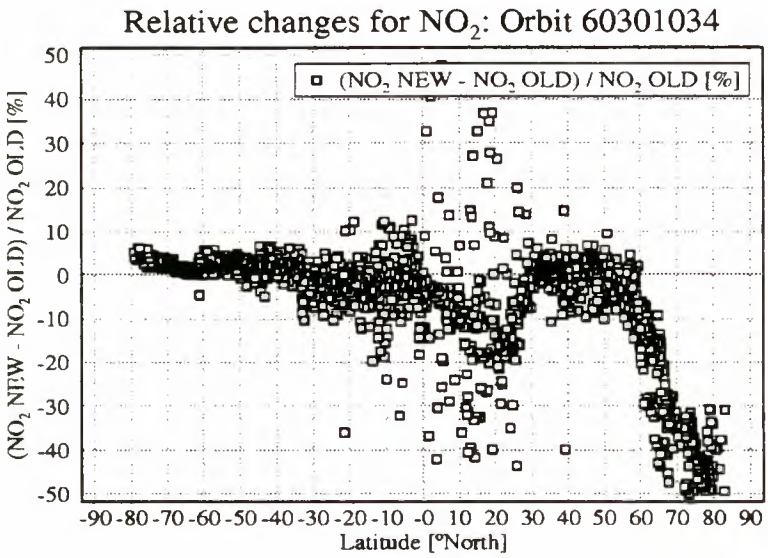
Relative changes for NO2: Orbit 60301034
(NO2 NEW - NO2 OLD) / NO2 OLD [%]
(NO2 NEW - NO2 OLD) / NO2 OLD [%]
50
40
30
20
10
0
-10
-20
-30
-40
-50
-90 -80 -70 -60 -50 -40 -30 -20 -10 -0 10 20 30 40 50 60 70 80 90
Latitude [°North]

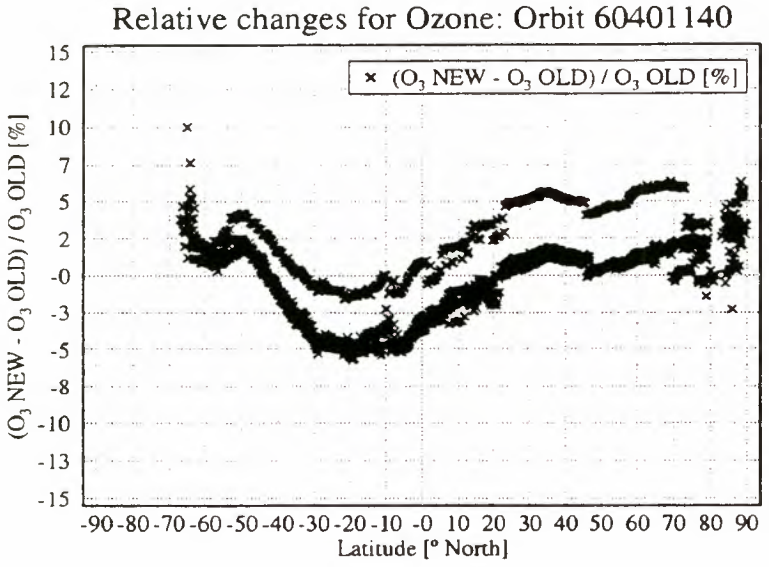
Relative changes for Ozone: Orbit 60401140
(O3 NEW - O3 OLD) / O3 OLD [%]
(O3 NEW - O3 OLD) / O3 OLD [%]
15 12 10 7 5 2 -0 -3 -5 -8 -10 -13 -15
-90 -80 -70 -60 -50 -40 -30 -20 -10 -0 10 20 30 40 50 60 70 80 90
Latitude [° North]

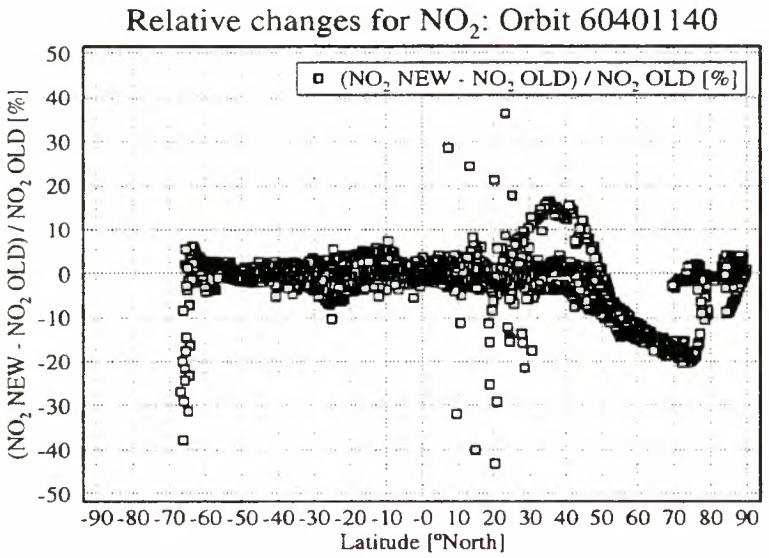
Relative changes for NO2: Orbit 60401140
(NO2 NEW - NO2 OLD) / NO2 OLD [%]
(NO2 NEW - NO2 OLD) / NO2 OLD [%]
50 40 30 20 10 0 -10 -20 -30 -40 -50
-90 -80 -70 -60 -50 -40 -30 -20 -10 -0 10 20 30 40 50 60 70 80 90
Latitude [°North]

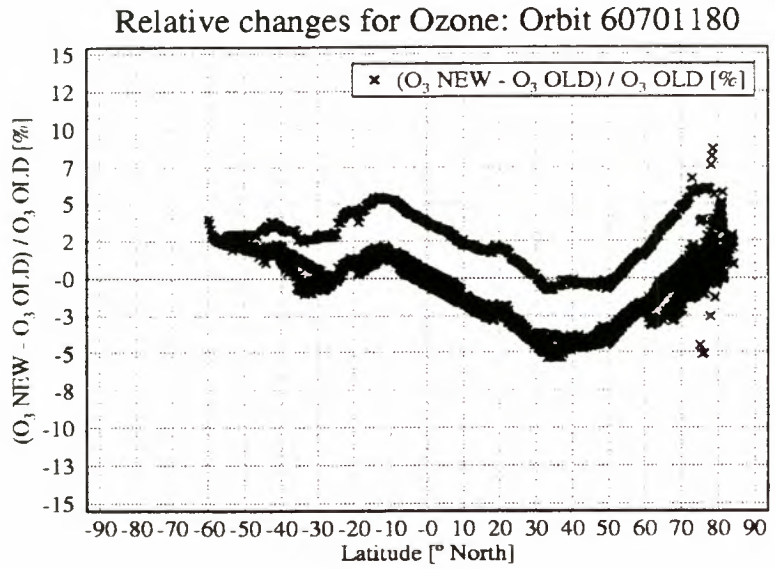
Relative changes for Ozone: Orbit 60701180
(O3 NEW - O3 OLD) / O3 OLD [%]
(O3 NEW - O3 OLD) / O3 OLD [%]
15 12 10 7 5 2 -0 -3 -5 -8 -10 -13 -15
-90 -80 -70 -60 -50 -40 -30 -20 -10 -0 10 20 30 40 50 60 70 80 90
Latitude [° North]

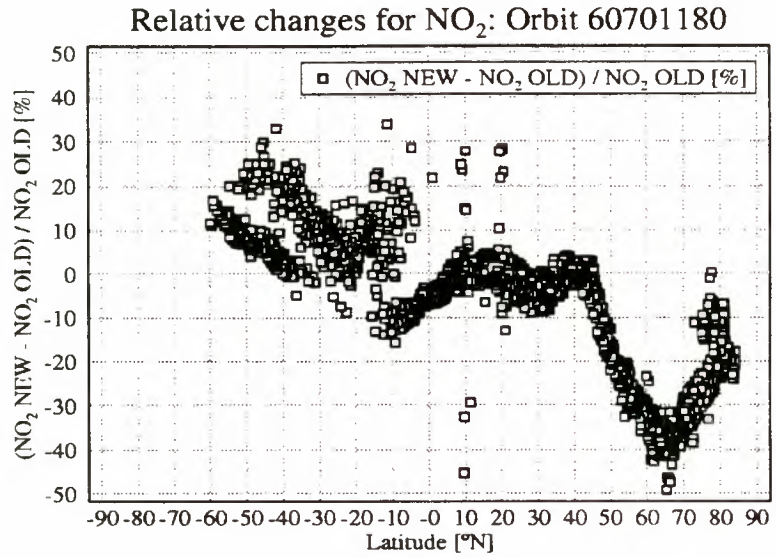
Relative changes for NO2: Orbit 60701180
(NO2 NEW - NO2 OLD) / NO2 OLD [%]
(NO2 NEW - NO2 OLD) / NO2 OLD [%]
50 40 30 20 10 0 -10 -20 -30 -40 -50
-90 -80 -70 -60 -50 -40 -30 -20 -10 -0 10 20 30 40 50 60 70 80 90
Latitude [°N]

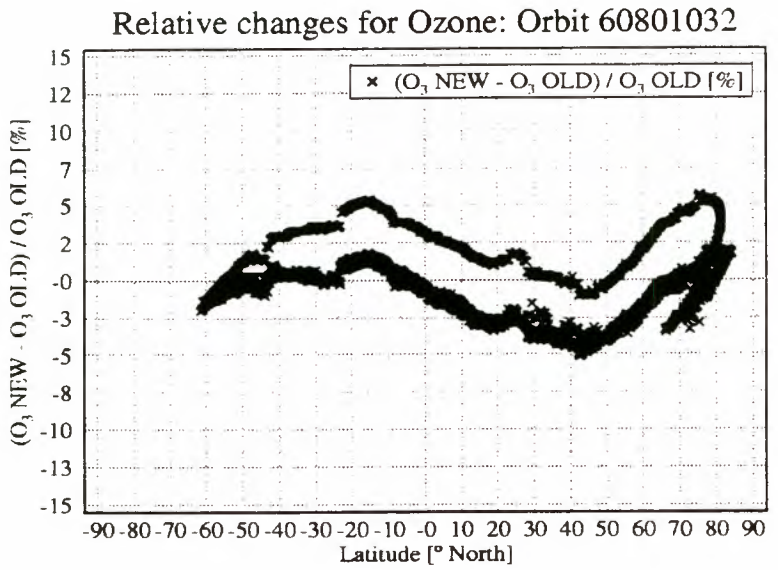
Relative changes for Ozone: Orbit 60801032
× (O3 NEW - O3 OLD) / O3 OLD [%]
(O3 NEW - O3 OLD) / O3 OLD [%]
15 12 10 7 5 2 -0 -3 -5 -8 -10 -13 -15
-90 -80 -70 -60 -50 -40 -30 -20 -10 -0 10 20 30 40 50 60 70 80 90
Latitude [° North]

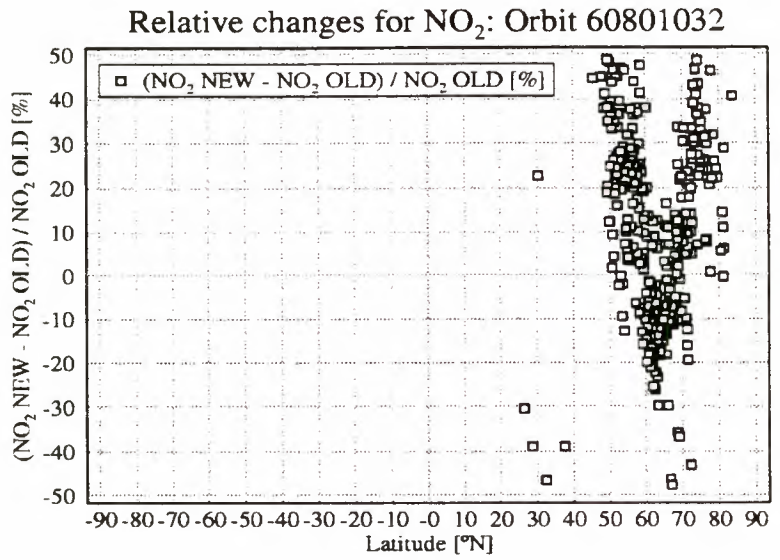
Relative changes for NO2: Orbit 60801032
(NO2 NEW - NO2 OLD) / NO2 OLD [%]
(NO2 NEW - NO2 OLD) / NO2 OLD [%]
50 40 30 20 10 0 -10 -20 -30 -40 -50
-90 -80 -70 -60 -50 -40 -30 -20 -10 -0 10 20 30 40 50 60 70 80 90
Latitude [°N]

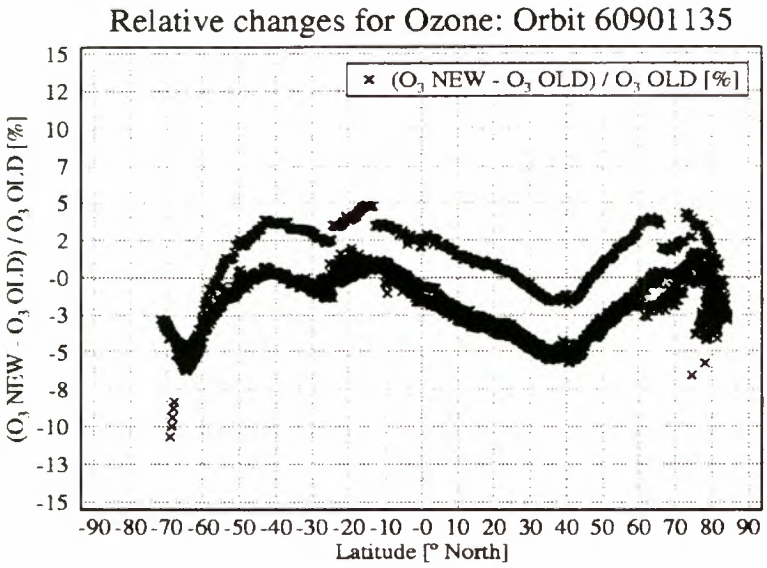
Relative changes for Ozone: Orbit 60901135
(O3 NEW - O3 OLD) / O3 OLD [%]
(O3 NEW - O3 OLD) / O3 OLD [%]
15
12
10
7
5
2
-0
-3
-5
-8
-10
-13
-15
-90 -80 -70 -60 -50 -40 -30 -20 -10 -0 10 20 30 40 50 60 70 80 90
Latitude [° North]

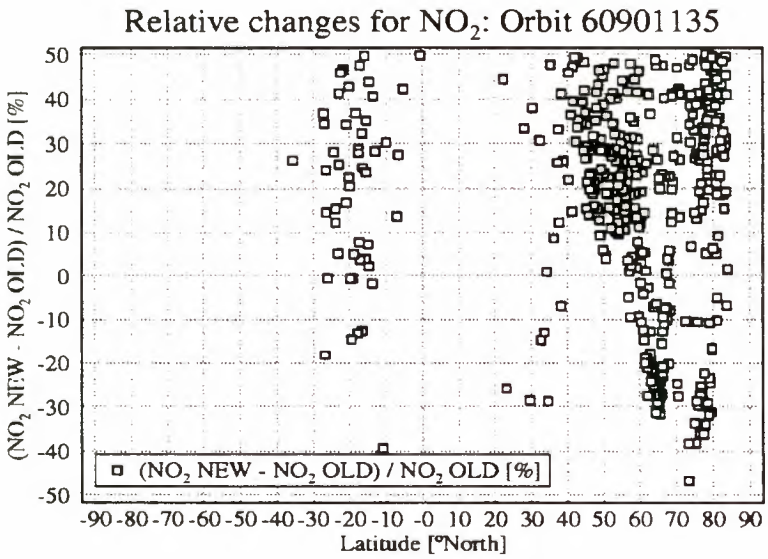
Relative changes for NO2: Orbit 60901135
(NO2 NEW - NO2 OLD) / NO2 OLD [%]
(NO2 NEW - NO2 OLD) / NO2 OLD [%]
50
40
30
20
10
0
-10
-20
-30
-40
-50
-90 -80 -70 -60 -50 -40 -30 -20 -10 -0 10 20 30 40 50 60 70 80 90
Latitude [°North]

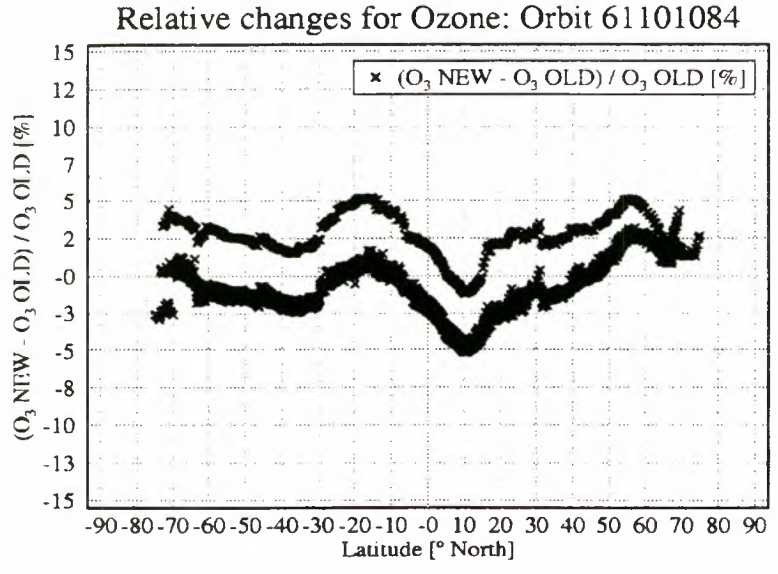
Relative changes for Ozone: Orbit 61101084
(O3 NEW - O3 OLD) / O3 OLD [%]
(O3 NEW - O3 OLD) / O3 OLD [%]
15 12 10 7 5 2 -0 -3 -5 -8 -10 -13 -15
-90 -80 -70 -60 -50 -40 -30 -20 -10 -0 10 20 30 40 50 60 70 80 90
Latitude [° North]

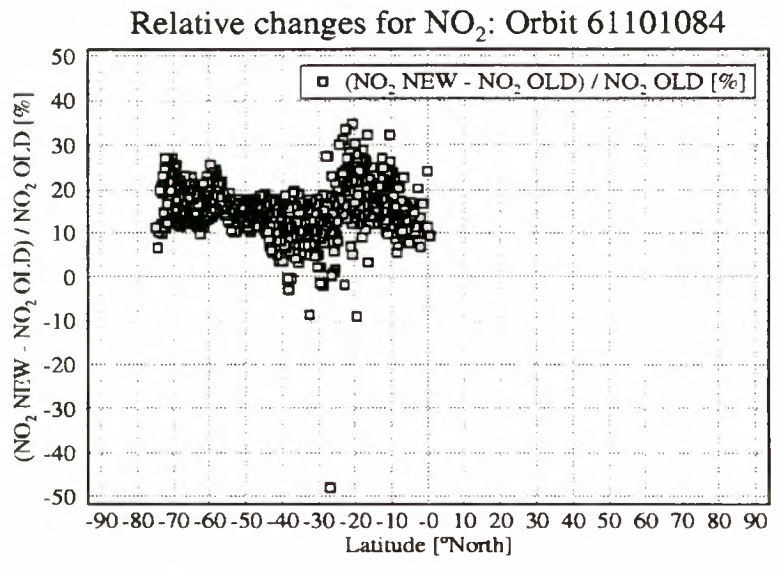
Relative changes for NO2: Orbit 61101084
(NO2 NEW - NO2 OLD) / NO2 OLD [%]
(NO2 NEW - NO2 OLD) / NO2 OLD [%]
50 40 30 20 10 0 -10 -20 -30 -40 -50
-90 -80 -70 -60 -50 -40 -30 -20 -10 -0 10 20 30 40 50 60 70 80 90
Latitude [°North]

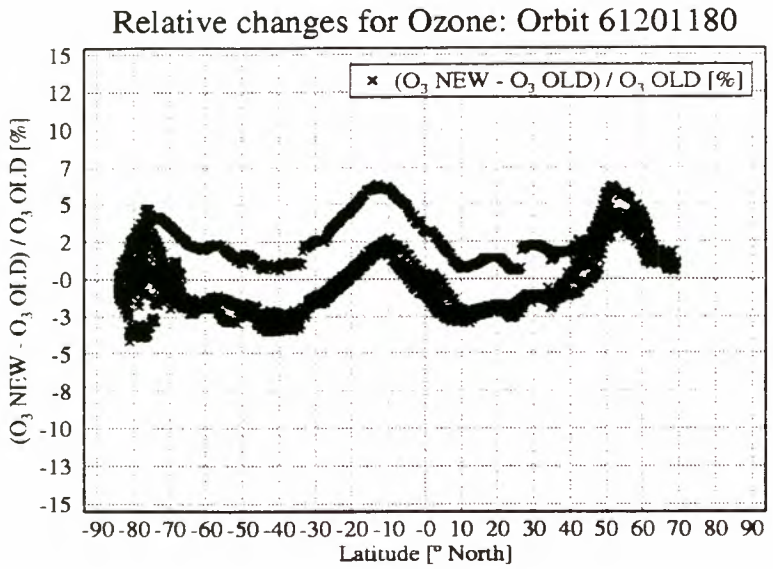
Relative changes for Ozone: Orbit 61201180
(O3 NEW - O3 OLD) / O3 OLD [%]
(O3 NEW - O3 OLD) / O3 OLD [%]
15 12 10 7 5 2 -0 -3 -5 -8 -10 -13 -15
-90 -80 -70 -60 -50 -40 -30 -20 -10 -0 10 20 30 40 50 60 70 80 90
Latitude [° North]

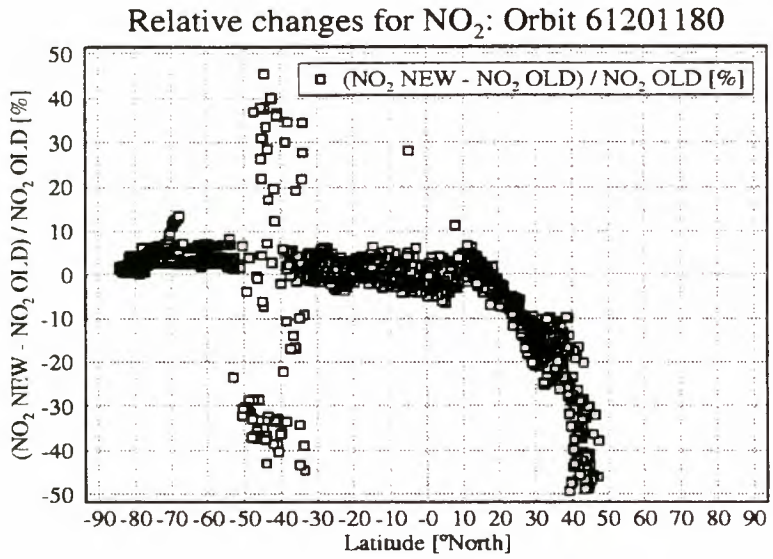
Relative changes for NO2: Orbit 61201180
(NO2 NEW - NO2 OLD) / NO2 OLD [%]
(NO2 NEW - NO2 OLD) / NO2 OLD [%]
50 40 30 20 10 0 -10 -20 -30 -40 -50
-90 -80 -70 -60 -50 -40 -30 -20 -10 -0 10 20 30 40 50 60 70 80 90
Latitude [°North]

Annex: 2

Table 1: Orbits used for the comparison of version 2.0 and 2.3 data.

60101102
60201204
60301034
60401140
60701180
60801032
60901135
61101084
61201180

Annex: 3

Table 2: Dates with new GOME measurements above Bremen.

01.01.1996	07.03.1996	08.03.1996	20.04.1996
11.05.1996	12.05.1996	21.05.1996	10.07.1996
16.07.1996	24.07.1996	07.08.1996	28.08.1996
29.08.1996	20.09.1996	11.10.1996	02.11.1996
03.11.1996	24.11.1996	16.12.1996	17.12.1996
27.12.1996	05.01.1997	07.02.1997	

Table 3: Dates with new GOME measurements above Ny-Ålesund

15.02.1996	05.03.1996	07.03.1996	08.03.1996
10.03.1996	28.03.1996	29.03.1996	30.03.1996
31.03.1996	01.04.1996	02.04.1996	04.04.1996
06.04.1996	07.04.1996	19.04.1996	20.04.1996
21.04.1996	22.04.1996	23.04.1996	25.04.1996
27.04.1996	29.04.1996	12.05.1996	13.05.1996
14.05.1996	16.05.1996	17.05.1996	18.05.1996
19.05.1996	20.05.1996	21.05.1996	06.06.1996
08.06.1996	09.06.1996	10.06.1996	11.06.1996
13.06.1996	24.06.1996	25.06.1996	27.06.1996
28.06.1996	29.06.1996	01.07.1996	02.07.1996
03.07.1996	04.07.1996	10.07.1996	16.07.1996
17.07.1996	18.07.1996	19.07.1996	20.07.1996
22.07.1996	23.07.1996	24.07.1996	25.07.1996
07.08.1996	08.08.1996	09.08.1996	10.08.1996
11.08.1996	12.08.1996	13.08.1996	14.08.1996
15.08.1996	16.08.1996	28.08.1996	29.08.1996
30.08.1996	31.08.1996	01.09.1996	02.09.1996
03.09.1996	04.09.1996	05.09.1996	06.09.1996
20.09.1996	21.09.1996	22.09.1996	23.09.1996
24.09.1996	25.09.1996	26.09.1996	12.10.1996
13.10.1996	15.10.1996		

Geophysical comparison of the GOME Data Processors GDP 2.0 and 2.3 by means of ground-based networks

J.-C. Lambert and P.C. Simon

Institut d'Aéronomie Spatiale de Belgique (IASB-BIRA)
Avenue Circulaire 3, B-1180 Bruxelles
E-mail: lambert@bira-iasb.oma.be

Geophysical comparison of the GOME Data Processors GDP 2.0 and 2.3 by means of ground-based networks

J.-C. Lambert and P.C. Simon

1. Introduction

This document reports on investigations carried out at IASB-BIRA in the frame of the preliminary validation of the version 2.3 of the GOME Data Processor Level 1-to-2. The results and conclusions were presented at the GOME Tiger Team II Meeting held on 14 January 1998 at DLR (Oberpfaffenhofen, Germany).
After a summary of the current conclusions on GDP 2.0 drawn from previous and ongoing ground-based validation studies, the performances of GDP 2.3 for total ozone and nitrogen dioxide retrieval are analysed with respect to those of GDP 2.0 by means of ground-based observations from the Network for the Detection of Stratospheric Change (NDSC). The geophysical relevance of GOME data is emphasised. Conclusions and recommendations are given concerning the future processing of GOME level-2 data and possible improvements of the GDP.

2. Current performances of GDP 2.0

2.1. Total ozone

A combined validation of total ozone measured since June 1996 by GOME, TOMS-EP and TOMS-AD has been carried out by means of ground-based observations from the pole-to-pole SAOZ/UV-visible network and from Dobson and Brewer spectrophotometers operating at selected sites of the NDSC Alpine and Antarctic stations. The study demonstrates a good average agreement to within ±2-4% between all space-borne and ground-based instruments at northern middle latitude. A small shift is detected in GOME data on December 31, 1996. At high latitude, in both hemispheres, the mean agreement and the scatter vary with the solar zenith angle (SZA) of the space observation, largely due to the retrieval method and its sensitivity to errors in the ozone profile shape derived from a seasonal climatology. The dispersion of satellite data increases significantly beyond 85° SZA. The GOME total ozone increases systematically beyond 80° SZA, however its average SZA dependence is dominated by a seasonal variation resulting in positive mean deviations beyond 80° SZA in winter-spring and in negative mean deviations beyond 65-70° SZA in summer-fall. The agreement between the GOME and the ground-based total ozone also depends on the ozone column, indicative of a difference of sensitivity. In particular, low ozone columns are overestimated by the GOME by a few percent at the tropics and by more under springtime ozone depletion.
Although a SZA dependence is also present in the TOMS data, its amplitude is smaller than that of the GOME, does not vary with the season, and is not significant below 80°. However, TOMS data are found to overestimate ground-based data in the southern hemisphere. A difference of sensitivity is not clearly observed with the TOMS, except at the southern tropic.

2.2 Total nitrogen dioxide

GOME total NO_2 retrieved routinely with GDP 2.0 since June 1996, has been compared to observations from the SAOZ/UV-visible network. Outside the period from July 29 to October 15, 1996, when a strong wavelength registration shift in GOME spectral channel 3 made the NO_2 retrieval irrelevant, GOME NO_2 data are consistent, although scattered, especially in polluted areas. This scatter originates partly in the high sensitivity of the GOME observation (nadir geometry) to the tropospheric NO_2 content - which can exhibit sharp gradients - compared to the ground-based zenith-sky observations at twilight. Day-to-day fluctuations of GOME total NO_2 generally are reasonable, but the comparison from pole to pole with SAOZ data shows that the mean agreement depends clearly

on the latitude, the season and the SZA. This seasonal and latitudinal dependence arises mainly from the NO_2 vertical distributions used in the NO_2 retrieval of GDP 2.0, derived from the MPI 2D atmospheric chemical transport model. In some cases, those profiles are found inconsistent with real NO_2 density profiles measured with SAOZ-balloon sondes. Test case studies were performed using GOME total NO_2 retrieved with other NO_2 profiles, more consistent with SAOZ-balloon data : the US Standard profile, now implemented in GDP 2.3, and that measured during the Map Globus campaign in 1983. Those studies showed a better general agreement between the GOME and SAOZ total NO_2, and a better geophysical consistency.

3. Validation data sets

The present study is based on pole-to-pole ground-based data provided by 24 instruments associated to the NDSC. Total ozone is that measured by 16 SAOZ and SAOZ-like UV-visible DOAS spectrometers and by 8 Dobson/Brewer spectrophotometers, listed in Table 9-1. The 16 UV-visible spectrometers provide total nitrogen dioxide as well. Complementary information is provided by ozonesondes, lidars, ECMWF, and 3D chemical transport models.

Table 3.1 *Ground-based instruments contributing to the present study*

Station	Latitude	Longitude	Instrument	Responsible Institution
Ny-Ålesund	79 N	12 E	UV-visible (2)	NILU
Thulé	77 N	69 W	UV-visible	DMI
Scoresbysund	70 N	22 W	UV-visible	CNRS/DMI
Sodankylä	67 N	27 E	UV-visible	CNRS/FMI
Zhigansk	67 N	123 E	UV-visible	CNRS/CAO
Harestua	60 N	10 E	UV-visible	IASB-BIRA
Aberystwyth	52 N	4 W	UV-visible	Uni. Wales
Hohenpeißenberg	48 N	11 E	Dobson, Brewer	Deutsche Wetterdienst
Jungfraujoch	47 N	8 E	UV-visible	IASB-BIRA
Arosa	46 N	9 E	Dobson, Brewer	ETH-Zürich
Bordeaux	46 N	1 W	Dobson	Uni. Bordeaux
Haute Provence	44 N	6 E	UV-visible, Dobson	CNRS
Tarawa	1 N	173 E	UV-visible	CNRS
Saint Denis	21 S	55 E	UV-visible	Uni. de La Réunion
Bauru	22 S	49 W	UV-visible	CNRS/UNESP
Kerguelen	49 S	70 E	UV-visible	CNRS
Vernadsky/Faraday	65 S	64 W	Dobson	BAS
Dumont d'Urville	67 S	140 E	UV-visible	CNRS
Rothera	68 S	68 W	UV-visible	BAS
Halley	76 S	26 W	Dobson	BAS

A GOME level-2 validation data set of about 330 orbits has been processed with GDP 2.3, including every 15th orbit acquired in 1996. Following the current conclusions on GDP 2.0, 36 additional orbits have been selected for processing in order to test improvements of the GDP under special conditions and to identify possible changes in the column-resolved SZA dependence of GOME. Those special orbits are listed in Tables 9-2 to 9-5.

Table 3.2 *Orbits selected for comparison between mid-morning and midnight Sun GOME data*

Antarctic summer : Dumont d'Urville		**Arctic summer : Sodankylä**	
Mid-morning	Midnight Sun	Mid-morning	Midnight Sun
61227225	61227143	60710096	60710200
70117000	70117134	60724092	60724192
70117215			

Table 3.3 *Orbits selected for investigations on winter-spring data at the polar circles*

Antarctic springtime : Dumont d'Urville		**Arctic springtime : Sodankylä**	
Inside vortex	Outside vortex	Inside vortex	Outside vortex
60831225	60917222	70115093 (low T)	70118093
60902000	60917236	70122091 (low T)	70207105
60902215	61008230	70119090 (low O_3)	70207090
61026001		70122091 (low O_3)	
61026216			

Table 3.4 *Orbits selected for investigations on the difference of sensitivity in the southern hemisphere*

Southern Tropic : Bauru		**Southern middle latitude : Kerguelen**	
Low ozone	High ozone	Low ozone	High ozone
70322132	70427123	60709035	61109043
70429131	60903125	60718040	61226046

Table 3.5 *Orbits selected to investigate the New Year's shift of GOME data*

New Year's shift at the NDSC/Alpine stations			
61227111	61226115	70104116	70105112

4. Ground-based analysis of GDP 2.3

4.1. Total ozone

GOME total ozone data out of the level-2 validation set of 370 orbits have been compared to correlative ground-based observations. From pole to pole, the average agreement with GDP 2.3 is found similar to that observed with GDP 2.0. Changes often are within a few percent, that is within the accuracy level of ground-based measurements. When looking in more details at the influence of the cloud fraction or the AMF, it appears that

modifications to ICFA or to the AMF computation (e.g., new combined time/latitude interpolation scheme, multiple scattering look-up table computed with GOMETRAN v2.0, parabolic weighting of AMFs) in GDP 2.3 do not affect significantly the GOME total ozone and its agreement with ground-based observations. Due to the lack of GOME data at northern mid-latitude around December 31, 1996, investigations on the New Year's Alpine shift do not yield relevant results.

The seasonal SZA dependence of GOME at high latitude persists with GDP 2.3, in both hemisphere. In Figure 9-1, GOME data acquired in summer at mid-morning (descending orbit, moderate SZA) and under midnight Sun (ascending orbit, high SZA) are compared to SAOZ data at Sodankylä. This figure shows a similar summer SZA dependence for both GDP 2.0 and 2.3. The winter SZA dependence at Sodankylä is illustrated in Figure 9-2, showing no significant improvement. For both seasons, a small 'rotation' of the SZA dependence is observed, with higher ozone at low SZA and lower ozone at high SZA, but no significant improvement is to date. Figure 9-2 also shows that the SZA dependence is still column-resolved. Investigations in the Tropics, at southern middle latitude and under springtime ozone depletion in both the Arctic and the Antarctic confirm that

the difference of sensitivity of GOME remains. Additional investigations were carried out on the possible influence of PSCs or the effect produced by the change in the determination of the Bass-Paur temperature. However, those effects are masked by the strong SZA/column dependence and cannot be studied with the limited validation data set.

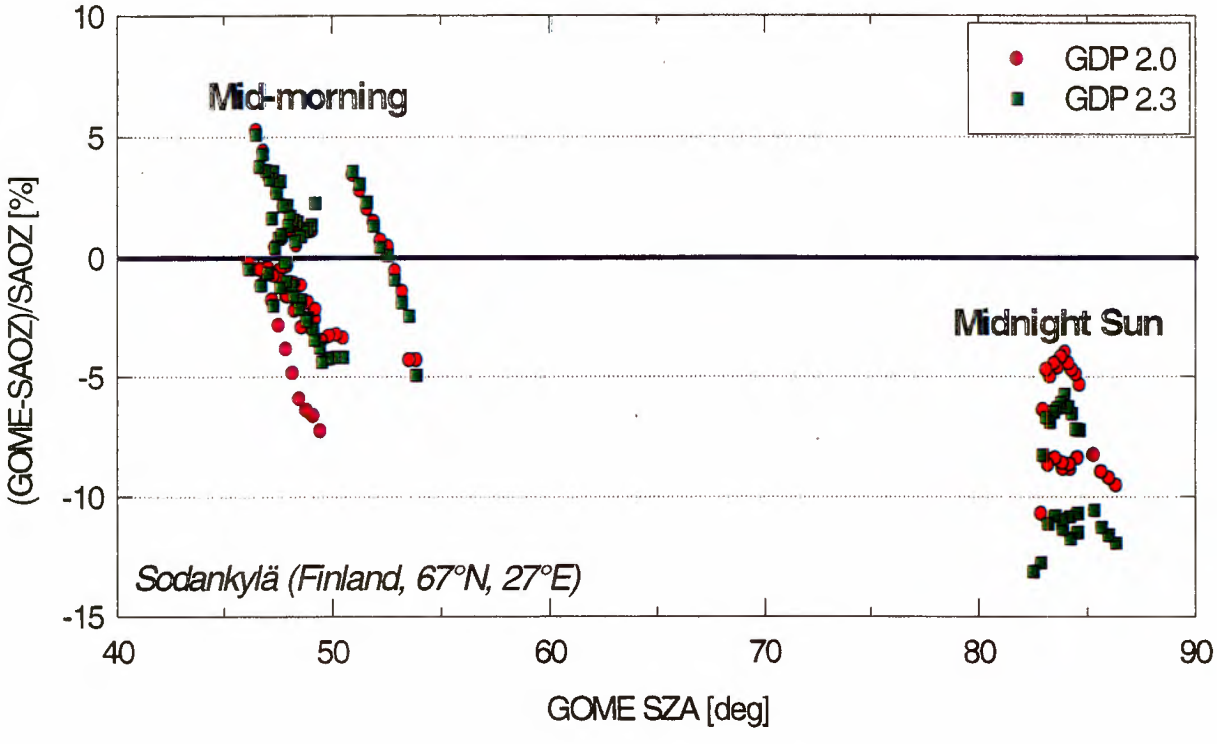

Figure 4.1 *Summer SZA dependence of the relative difference between the GOME and SAOZ total ozone in the Arctic : comparison between mid-morning (moderate SZA) and midnight Sun (high SZA) data at Sodankylä on July 10 and 24, 1996.*

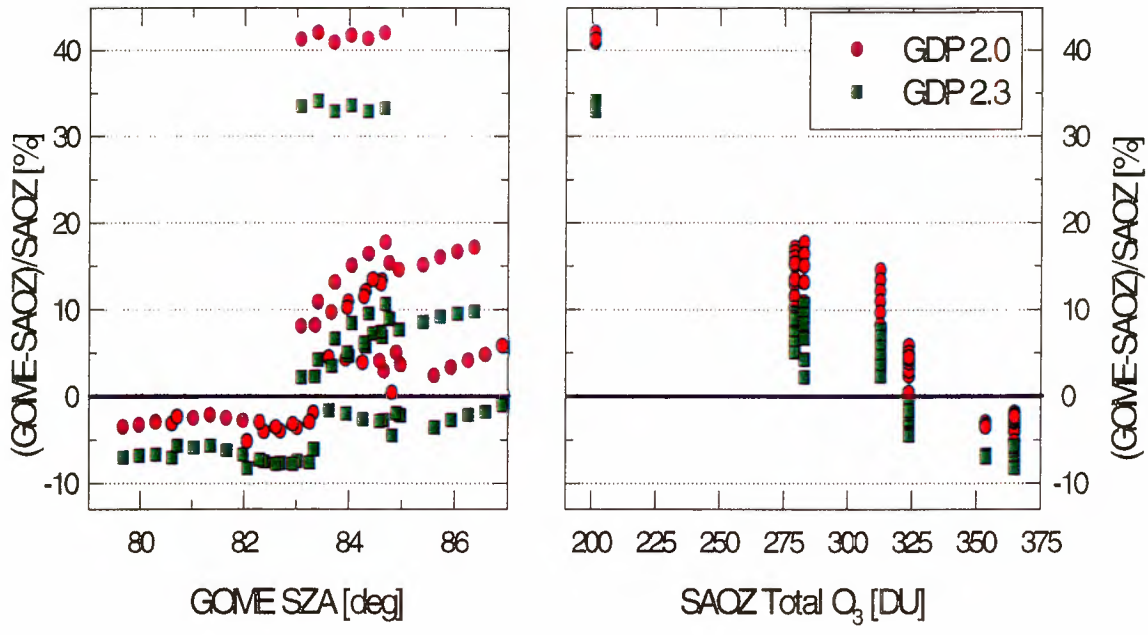

Figure 4.2 *Winter column-resolved SZA dependence of the relative difference between the GOME and SAOZ total ozone in the Arctic : comparison at Sodankylä for 7 days in January and February 1997.*

4.2. Total nitrogen dioxide

The 370 orbits of the level-2 validation data set have been analysed with respect to ground-based observations and modelling results. A special care has been given to the 36 additional orbits representing special conditions. The data set of GOME total NO_2 is found to be 'cleaner' with GDP 2.3 than with GDP 2.0. The occurrence of anomalous values of total column beyond 10 x 10^{15} molec.cm^{-2} - and even beyond 100 x 10^{15} molec.cm^{-2} in extreme cases - is reduced by a large factor, and errors on the DOAS fit, given in the level-2 data files, look more reasonable. Due to the limited data set, it is difficult to estimate the relevance of the day-to-day variation, but the scatter between adjacent ground pixels is reasonable according to the sensitivity of GOME to the troposphere. There are less unreasonable scenes with enhanced pollution. In general, the geophysical consistency of GOME total NO_2 retrieved with GDP 2.3 is improved. The seasonal and latitudinal variations of GOME NO_2 are in much better agreement with ground-based observations. Figure 9-3 illustrates the improvement of both total NO_2 and its scatter along track for an individual orbit in the Tropics and at middle latitude. Figure 9-4 shows in Eastern Siberia that GDP 2.3 yields more realistic values of total NO_2 in unpolluted regions. Figure 9-5 shows that the inconsistent sharp increase of total NO_2 towards the pole is reduced down to a more natural slope, but the anomalous behaviour under midnight Sun conditions persists. The general improvement is attributed mainly to the use of the NO_2 vertical distribution from US Standard climatology, which was recommended in a previous study as a first step towards a geophysically consistent NO_2 product. E.g., the reduction of the NO_2 column in Siberia observed in figure 9-4 is related to the relevant reduction in tropospheric content of the US Standard climatology compared to that of the MPI profiles used in GDP 2.0. Although the benefit of GDP 2.3 compared to GDP 2.0 is clear, it must be kept in mind that several major source of uncertainties remain, and significant improvements of the GDP are still required for total NO_2.

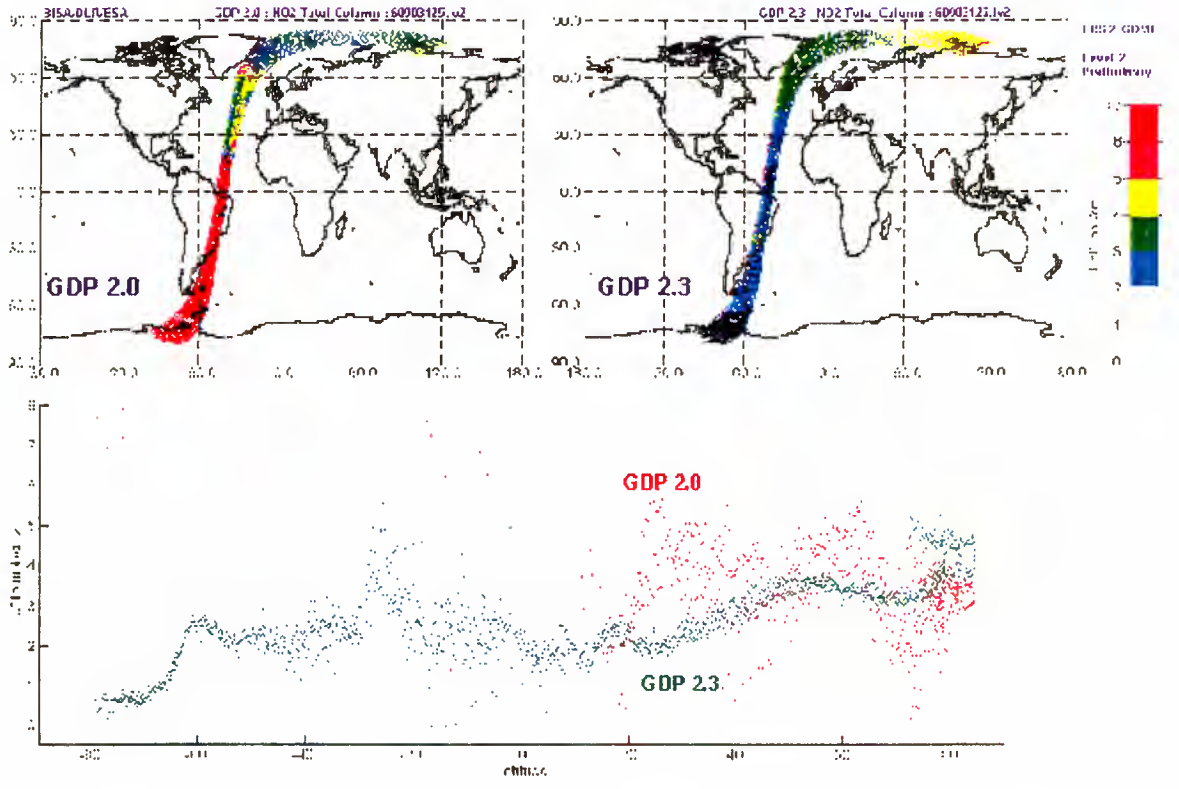

Figure 4-3 *Comparison of GOME NO_2 vertical column for an individual orbit (61109043.lv2) retrieved with GDP 2.0 and GDP 2.3. In Eastern Siberia, GDP 2.3 yields more realistic NO_2 values for an unpolluted region. The picture also shows GDP 2.3 data obtained with the polar viewing mode processing.*

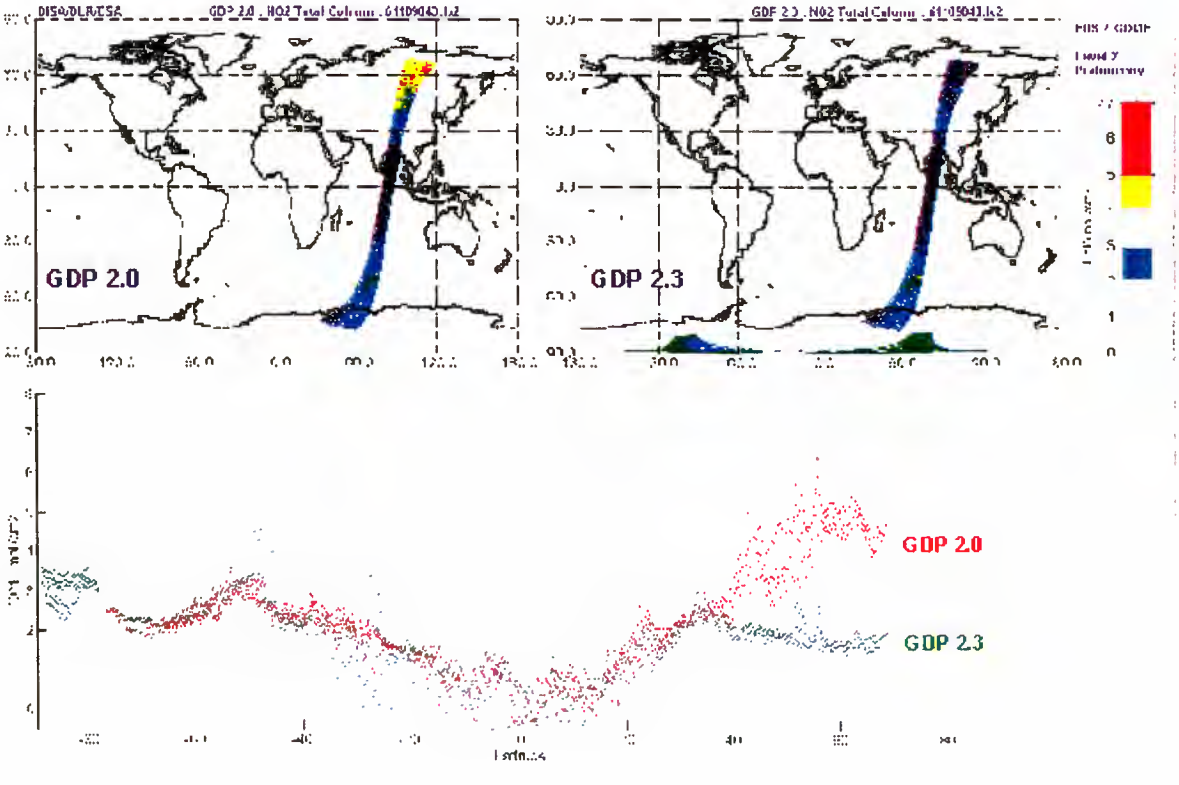

Figure 4-4 *Comparison of GOME NO_2 vertical column for an individual orbit (61109043.lv2) retrieved with GDP 2.0 and GDP 2.3. In Eastern Siberia, GDP 2.3 yields more realistic NO_2 values for an unpolluted region. The picture also shows GDP 2.3 data obtained with the polar viewing mode processing.*

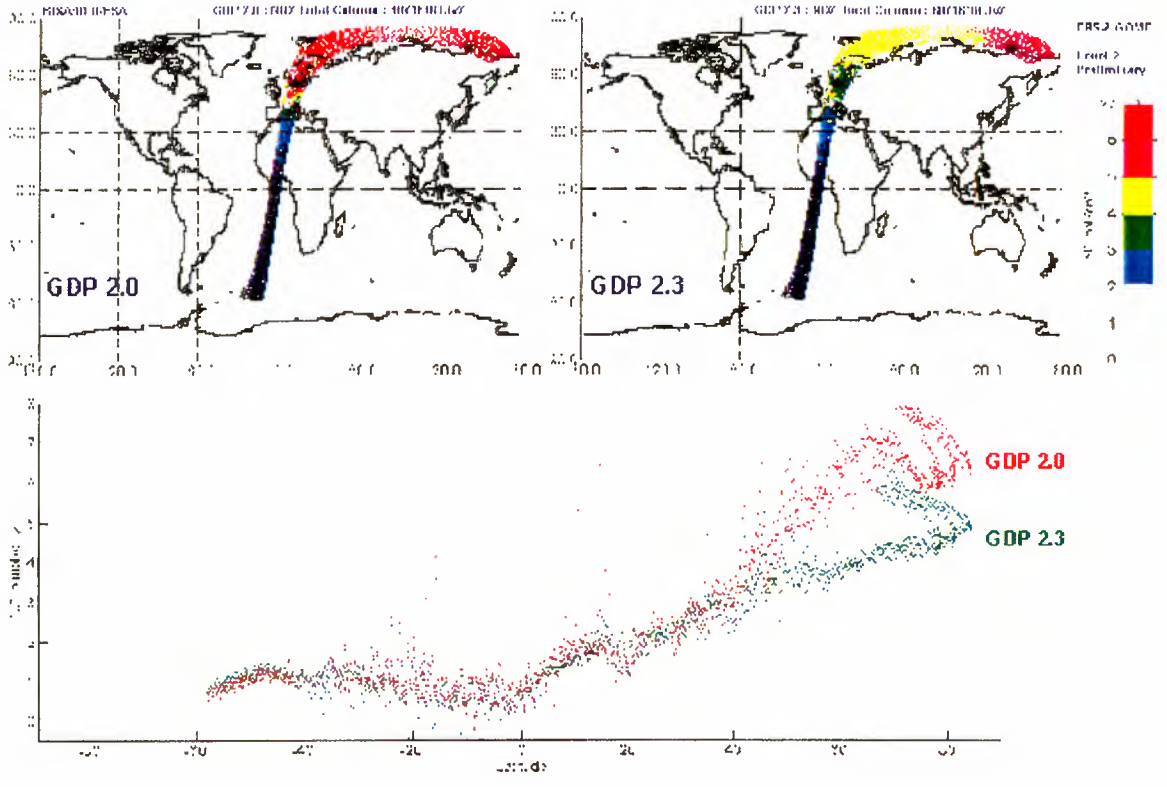

Figure 4-5 *Comparison of GOME NO_2 vertical column for an individual orbit (60716100.lv2) retrieved with GDP 2.0 and GDP 2.3 data in the Tropics and the northern hemishphere are less scattered. The inconsistent sharp increase of total NO_2 beyond 40°N towards the pole is reduced down to a more realistic slope, however anomalous behaviour under midnight Sun conditions persists.*

5. Conclusions and recommendations

While there is no major difference between GDP 2.0 and GDP 2.3 for total ozone retrieval, the improvement of the geophysical consistency of total NO_2 and the implementation of the polar viewing mode processing in GDP 2.3 vindicate its use for future GOME total ozone and NO_2 retrieval. However, it must be kept in mind that significant improvements are still needed for both total ozone and NO_2 data.

For total ozone retrieval, the same problems as detected with GDP 2.0 remain. Possible solutions are well identified. The use in GDP of the so-called 'modified DOAS' approach, as well as a column-resolved climatology based on real ozone profile measurements like that used in the TOMS algorithm, could reduce both the seasonal SZA dependence of the GOME and its difference of sensitivity. But before using a column-resolved climatology similar to that used by the TOMS, it is recommended to investigate more deeply the sensitivity of the GOME retrieval to the ozone profile shape errors as well as the inter-hemispheric shift in TOMS data.

For total NO_2 retrieval, it is recommended to revisit the NO_2 profile data base used in the AMF calculation. The sensitivity of GOME retrieval to the profile shape errors should be studied in detail, for both the troposphere and the stratosphere. Test case studies with a 3D model suggest that a 2D climatology might be inadequate for nadir observations, partly due to the sharp gradients of the tropospheric NO_2 field.

Acknowledgements

The authors would like to thank Michel Van Roozendael (IASB), Jean-Pierre Pommereau and Florence Goutail (Service d'Aéronomie du CNRS, France) for fruitful discussions, and the PIs and instrument operators associated to the NDSC for their kind co-operation. They greatly appreciate the computational and logistic support provided by Pierre Gerard and José Granville (IASB). This work has been funded by the Prodex ERS-2 Project 1.

Validation of GOME level 1 data of version 1.4

P. Stammes and R. B. A. Koelemeijer

Royal Netherlands Meteorological Institute (KNMI)
P.O. Box 201, 3730 AE De Bilt, The Netherlands

E-mail: stammes@knmi.nl

27 March, 1998

Validation of GOME level 1 data of version 1.4

P. Stammes and R. B. A. Koelemeijer

1. Introduction

The GOME level 1 data product mainly consists of radiance spectra of Earth pixels (in units of mW/m2/nm/sr) and irradiance spectra of the Sun (in mW/m2/nm) from 240 to 790 nm. These GOME level 1 data are the basis of level 2 data products (e.g. trace gas columns and profiles) and higher level data products. Therefore, determining the accuracy of level 1 data is important for assessing the accuracy of derived products.
In this paper we report on a validation of GOME Earth radiance data produced by the GOME Data Processor (GDP) version 1.4. A limited set of data was processed with this version for the GOME Validation Tiger Team II, which met in January 1998. We have focused on the validation of the polarisation correction of Earth radiances, since in the polarisation calculation a significant change with respect to the previous version (1.2) had taken place (Sect. 2). In addition, the channel-to-channel jumps were considered for co-added data. These jumps are due to the serial read-out of the spectral channels (see *Stammes et al., 1996*) (Sect. 3). We further considered some individual spectra, (Sect. 4). Conclusions are given in (Sect. 5).
Note: The operational version of the GDP is version 1.5. This version is identical to version 1.4, except for the "-j" option in the extraction software.

2. Polarisation correction

GOME is a polarisation-sensitive instrument. Because sunlight reflected by the Earth is in general polarised, the radiation detected by GOME depends on the polarisation of the incident light. This polarisation is measured by the Polarisation Measurement Devices (PMDs) in broad bands centered around three wavelengths: 350 nm, 490 nm, and 700 nm. The measured quantity is the fractional polarisation p, which is related to the Stokes parameters I and Q defined with respect to the local meridian plane as follows: p = (1-Q/I)/2. By pi we indicate p measured by PMDi, where i=1,2,3.
Polarisation correction is one of the calibration steps in the GDP level 0-1 processing, and is needed to obtain radiances from instrument signals. The polarisation correction factor C depends on the instrumental polarisation sensitivity (ETA), which is measured preflight, and the fractional polarisation p of the scene.

2.1. Correction for PMD spatial aliasing

The so-called *PMD spatial aliasing* is the effect on the level 1 data of the imperfect collocation of scenes observed with the spectral channels and the PMDs, due to the PMD read-out delay. In GDP version 1.2 the collocation error is 1/32-th of a ground pixel averaged over a spectral channel (for the co-added data). This causes an error in p over inhomogeneous (e.g. cloudy) scenes.
In GDP version 1.4 a correction for PMD spatial aliasing has been implemented, which is an improvement w.r.t. the previous GDP versions. Now the collocation error is zero instead of 32-th of a ground pixel averaged over a spectral channel. Therefore, p has changed between versions 1.2 and 1.4. In the following subsections we will show the main effects of this change.

We note that collocation of scenes observed by spectral channels and PMDs can *never* be perfect, because of instrument design. Furthermore, for non-co-added data with 0.375 s integration time (July 1995 - March 1996) spatial aliasing is 4 times larger than for co-added data which have a 1.5 s integration time.

2.2. Effect on fractional polarisation

We have studied GOME polarisation data from orbit 9424 of 7 Feb 1997 (file: 70207104.lv1), which is shown in Fig. 1.

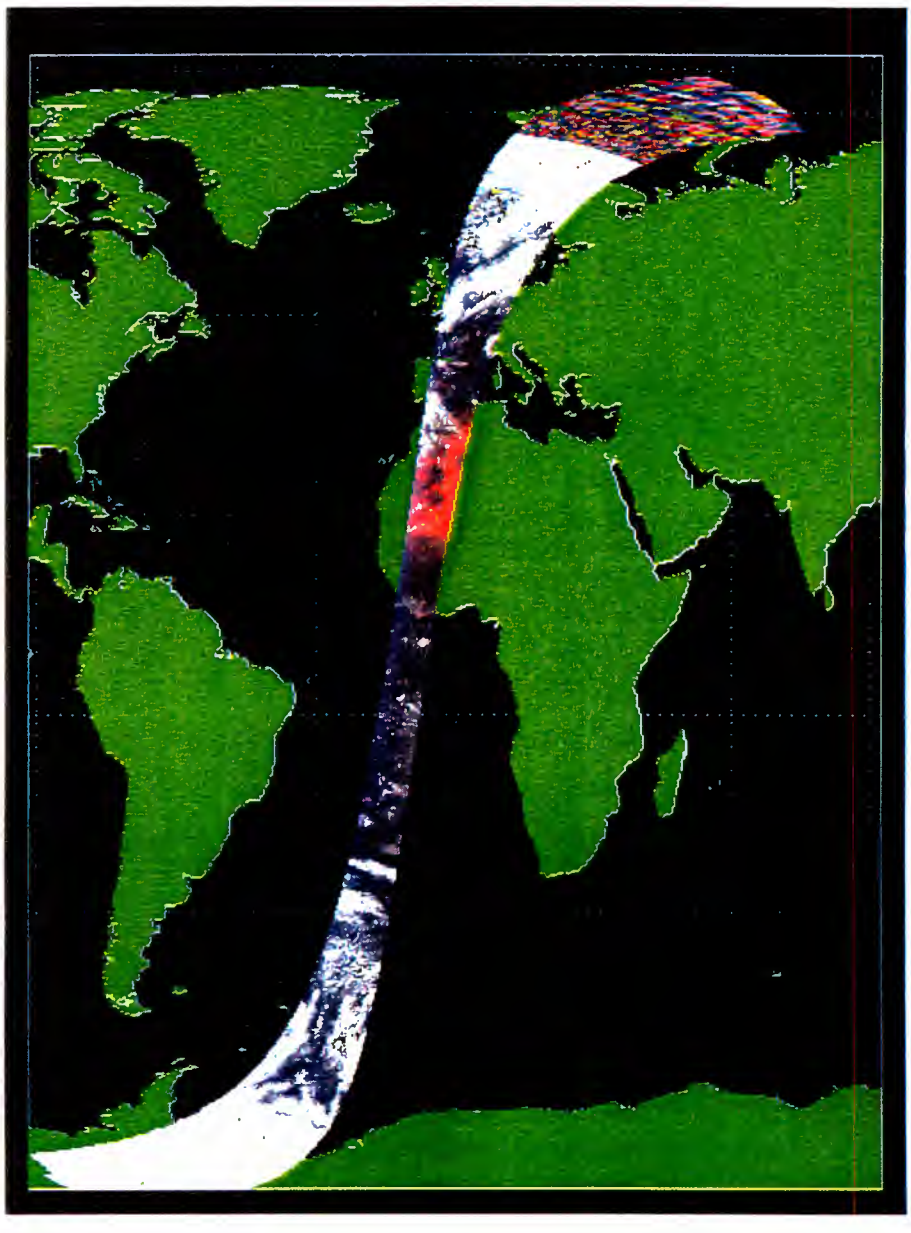

Figure 1: *PMD three-colour image of GOME orbit 9424 on 7 Feb 1997 (file: 70207104.lv1).*

In **Figure 2**, p3 is shown for the nadir pixels of this orbit. Clearly, in version 1.4 there are less peaks in p than in version 1.2, due to correction for PMD spatial aliasing. In **Figure 3**, the curves of Figure 2 are shown smoothed over 20 pixels to obtain the average behaviour of the curves. This shows that in version 1.4 not only the high frequency behaviour has changed, but also the average behaviour of the p curves along the orbit.

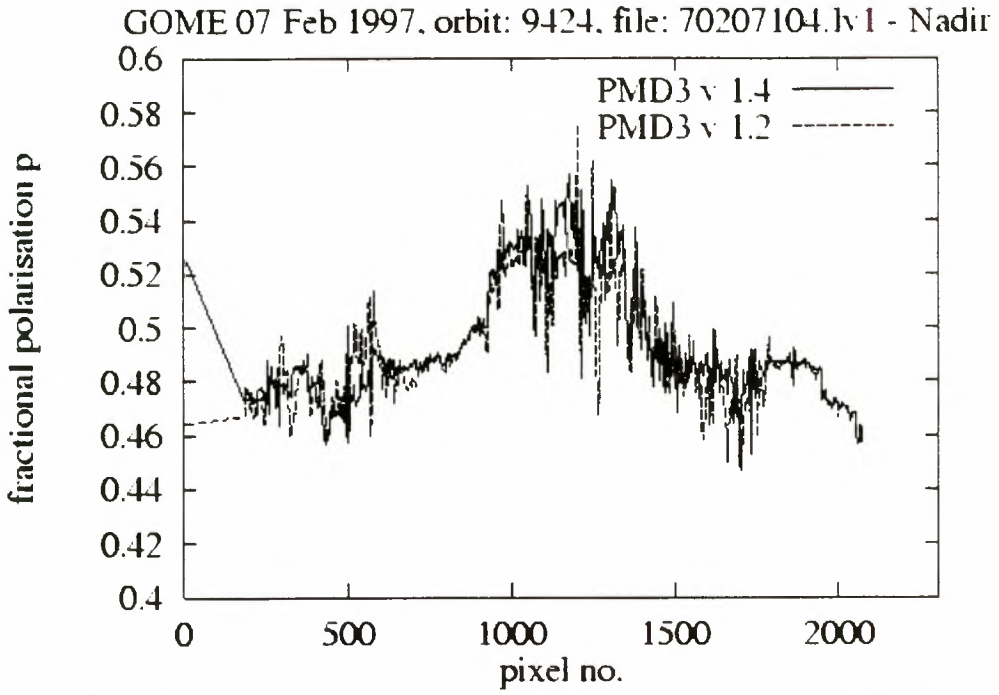

Figure 2: *Fractional polarisation p3 versus pixel number along orbit 9424 for two GDP versions.*

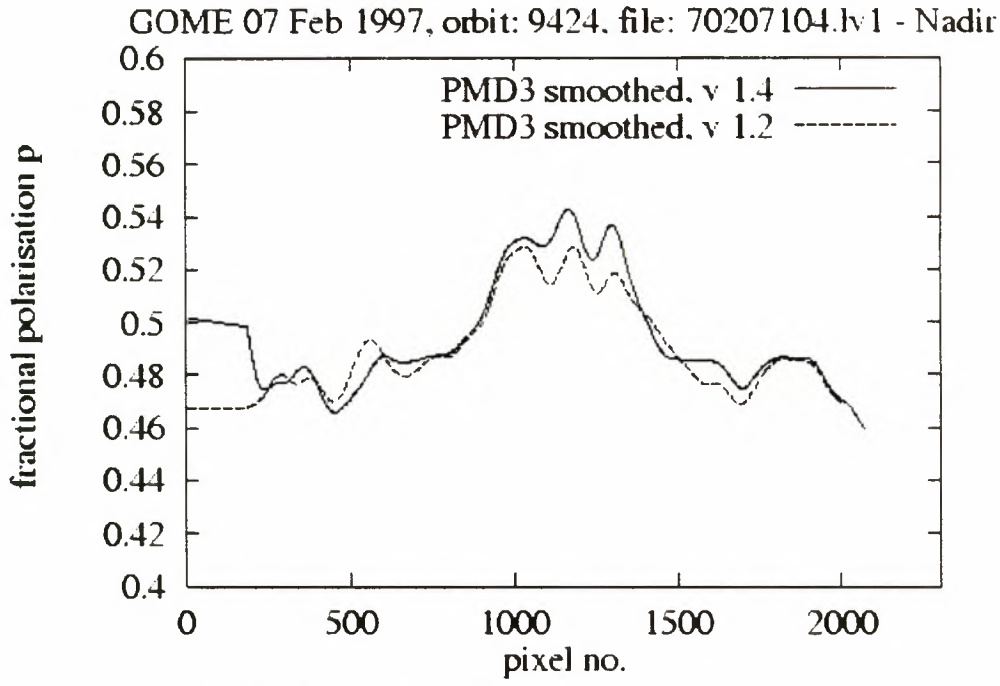

Figure 3: *Same as Fig. 2, but now the p values are smoothed over 20 pixels for two GDP versions.*

We note the following when comparing pi between version 1.4 and version 1.2:

- The differences are largest in p3 (around 700 nm), because clouds and surfaces are better visible at longer wavelengths.
- There are less and smaller peaks in p in version 1.4 than in version 1.2. The magnitude of peaks in p3 in version 1.2 could reach 0.05.
- The average value of p has changed, with typical (absolute) differences of 0.003 in p1, 0.01 in p2, and 0.02 in p3.

- The typical difference in the Rayleigh polarisation value (p0) is 0.002, due to geolocation changes.

Similar results were found for orbit 8938 (file: 70104115.lv1).

2.3. Effect on radiance

The polarisation correction factor C is influenced by a change in p. A change dp causes a relative change in C of dC/C, depending on ETA, which is strongly wavelength-dependent, and p itself. The resulting relative change in the radiance I is dI/I=dC/C. The differences in the radiances between version 1.4 and version 1.2 are typically, over an entire spectral channel and for the average of 20 pixels:

- in channels 1 and 2: dp=0.003 = dI/I= 0.15 %
- in channel 3: dp=0.01 = dI/I= 0.4 %
- in channel 4: dp=0.02 = dI/I= 0.8 %.

Considering individual pixels, the effect on the radiance can be several times larger; e.g., in channel 4 a typical change in p is about 0.05, which may cause a relative change in I of about 2 %.

2.4. Status of overlap polarisation

In the GOME validation phase (1995/96) the polarisation data from the spectral channel overlaps were found to be unreliable (*Stammes et al., 1996*). Here we found that the overlap polarisation data are also incorrect for the two orbits studied with co-added data, processed with GDP version 1.4. The channel 1/2 overlap polarisation at 313 nm is missing entirely, whereas the channel 3/4 overlap polarisation around 605 nm is deviating strongly from p3. The probable cause is that ETA is incorrect in the overlap regions, because for co-added data the channel-to-channel jumps are much smaller than for data from the validation phase (see Sect. 3).

2.5. Degradation of PMDs

Recently, it has been found by K. Bramstedt (Univ. Bremen, private communication, November 1997) that PMD1, operating in the UV, is degrading. For example, the fractional polarisation of sunlight should be 0.5. Indeed, in 1995 p1 was 0.5, but end of 1997 p1 was 0.456. This also means that the polarisation correction in the UV is deteriorating. In Fig. 4 it can be seen that indeed the p1 curve is not crossing the other p curves at p=0.5, which value should hold for a viewing geometry with polarisation angle 45 or 135 degrees (*Aben et al., 1997*). Presently, it is being investigated how to correct for this degradation of PMD1 (E. Hegels, DLR, private communication).

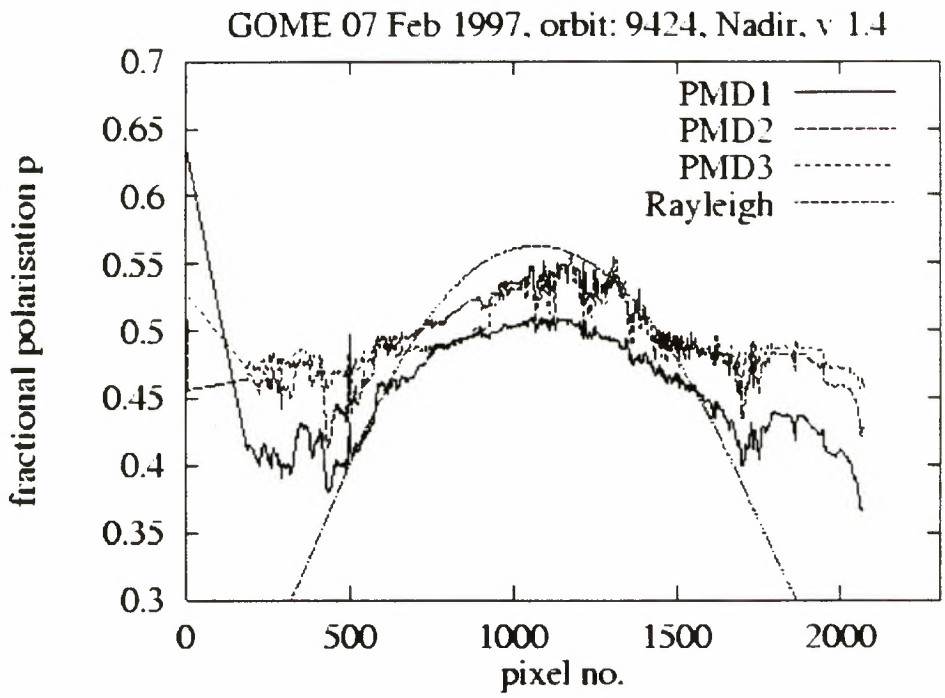

Figure 4: *Fractional polarisation of the 3 PMDs and the Rayleigh polarisation value for nadir pixels versus pixel number along orbit 9424 for GDP version 1.4.*

3. Channel-to-channel jumps

3.1. Magnitude of jumps

Channel-to-channel jumps are caused by inhomogeneities in the observed scene during the serial read-out of the diode arrays in 0.094 s. This effect is also known as spatial aliasing of the spectrum. Here we define a jump as the ratio of the radiance at the end of one channel to the radiance at the start of the next channel at the same wavelength. We consider as an example the jump of channel 3/channel 4 at 605 nm. Jumps should in principle be 4 times smaller with co-added data with integration time 1.5 s than with validation phase data when the integration time was 0.375 s (Jul 1995 - March 1996). In the validation phase, jumps were mostly in the range 0.80-1.20, but large excursions were also seen. As shown in Fig. 5, for co-added data the jumps are mostly in the range 0.95-1.05 (this holds for both orbits studied). These jumps are generally not pronounced and are not expected to confuse users. Actually, jumps can be helpful to detect scene inhomogeneity, which can be traced back to partial cloudiness or change of surface albedo.

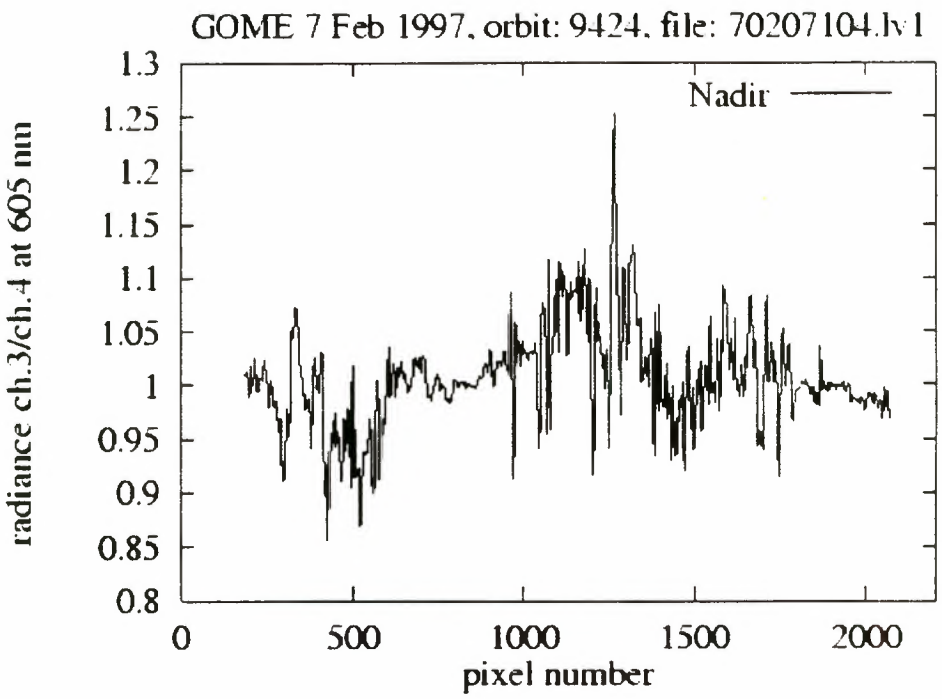

Figure 5: *Jumps from channel 3 to channel 4 at 605 nm along an orbit for the nadir pixels. GDP version 1.4.*

3.2. Jump correction

For the extraction software of version 1.4 a correction for the jumps was implemented with a calibration flag "J". However, this flag did not work for individual pixels. In the version 1.5 extraction software, there is now an option "-j" to correct for jumps. Correction for jumps means that the subpixel reflectivity information of the PMDs is used to scale the spectrum, and yield continuity at channel boundaries. However, this scaling is *physically incorrect*, because radiative transfer is a nonlinear process. Therefore, continuum and absorption bands cannot be multiplied with one factor. Furthermore, it is important to note that:

- jumps are *indicators* of the inhomogeneity of the scene
- jumps may be disguised as a *curvature* of the spectrum if the inhomogeneity is not at the extremes of a ground pixel
- the only places where the spectrum is *not* influenced by spatial aliasing, namely at each three wavelengths in channels 2, 3, and 4 where the diode numbers are identical, become corrupted by the jump correction.

4. Spectral noise in channel 3

From inspection of the spectra along orbit 9424, we found that from one pixel to the other the radiances in GOME channel 3 from about 400 to 450 nm may show a lot of noise (see Figs. 6 and 7). Apparently, the spectral calibration from 400 to 450 nm can become incorrect from one pixel to the other. It is known that the spectral calibration of GOME using the emission line lamp is sometimes causing problems, especially in the start of channel 3 (D. Loyola, DFD/DLR, private communication). This affects most seriously the retrieval of NO_2. Therefore, one should be cautious with using GOME spectra in this range.

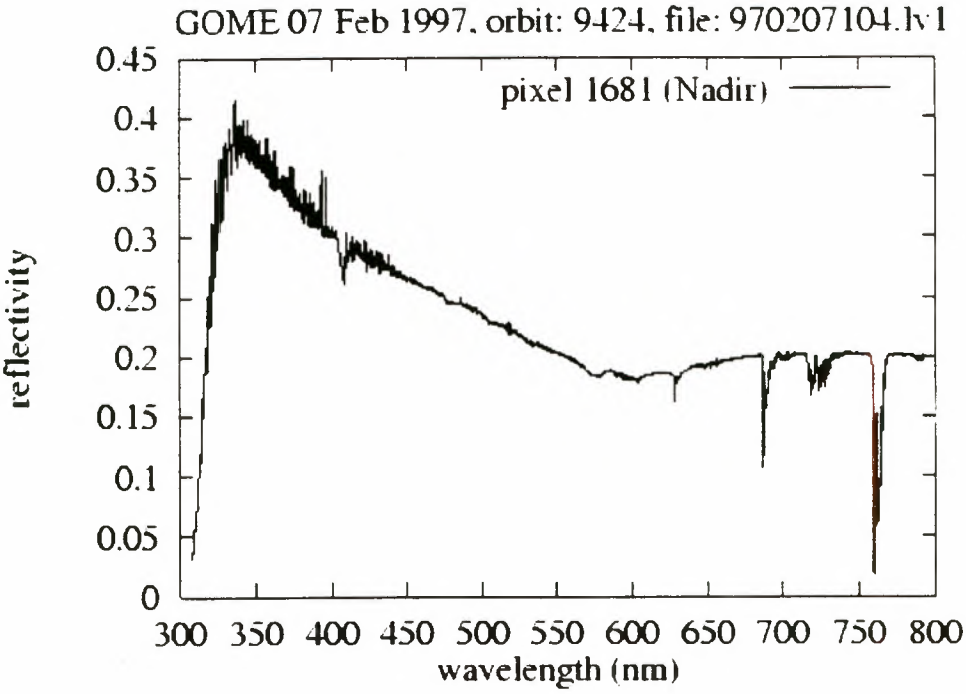

Figure 6: *Reflectivity spectrum of pixel 1681 of orbit 9424, situated over the Atlantic Ocean.*

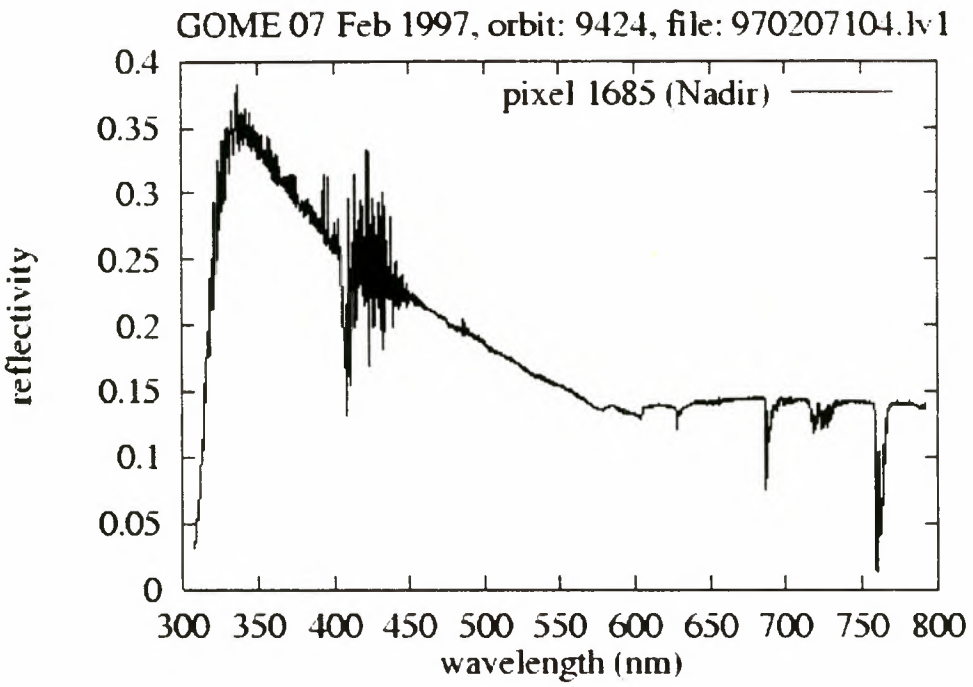

Figure 7: *Reflectivity spectrum of pixel 1685 of orbit 9424, which is adjacent to pixel 1681 shown in Fig. 6.*

5. Conclusions

The new GDP version 1.4 (almost equal to the operational version 1.5) is improved with respect to the problem of PMD spatial aliasing. The effect on the radiances of co-added orbits (after March 1996) is in general below 1 %, but can be a few percent for radiances in channel 4 in case of inhomogeneous (e.g. partly cloudy) scenes.

The channel-to-channel jumps are much smaller for the co-added data then they are for the validation phase data. Jump correction to make spectra look better is not generally required for these spectra.

Improvement of the GDP 0-1 algorithm is needed for:

- Correction for PMD1 degradation
- Interpolation of polarisation in UV
- Spectral calibration of channel 3.

References

Aben, I., D.M. Stam, and P. Stammes, "Polarisation validation method applied to GOME measurements", Proceedings of IRS '96, "Current Problems in Atmospheric Radiation", Eds. W.L. Smith and K. Stamnes, pp. 506-509, Deepak Publ., Hampton (VA) (1997)

Stammes, P., D.M. Stam, R.B.A. Koelemeijer, I. Aben, "Validation of GOME polarisation and radiance measurements", Proceedings of the GOME Validation Workshop, pp. 41-50, ESA, WPP-108 (1996)

Stammes, P., I. Aben, R.B.A. Koelemeijer, S. Slijkhuis, D.M. Stam, "GOME polarisation validation study", Proceedings of the Third ERS Symposium on "Space at the Service of our Environment", ESA SP-414, Vol. II, 669-674 (1997)

Validation of ICFA version 2.3

R. B. A. Koelemeijer and P. Stammes

Royal Netherlands Meteorological Institute (KNMI)
P.O. Box 201, 3730 AE De Bilt, The Netherlands
E-mail: koelemei@knmi.nl

27 March, 1998

Validation of ICFA version 2.3

R. B. A. Koelemeijer and P. Stammes

1. Introduction

This document describes the ICFA (Initial Cloud Fitting Algorithm) validation work performed at KNMI. We will describe validation results of two versions of ICFA: version 2.0, which used the rectangular slitfunction, and version 2.3, which uses the (physically more correct) simple hyperbolic slitfunction. In Section 2, we summarize the results of the ICFA 2.0 validation. ICFA 2.0 has been validated by comparing with cloud fractions derived from ATSR-2 data, and with cloud fractions from the ISCCP database. In Section 3, the differences between ICFA versions 2.0 and 2.3 are investigated by analysing data from 11 orbits acquired in September 1996. The relationship between ICFA 2.0 and 2.3 is used to make an update of the ICFA 2.0 validation results.

We stress that ICFA should produce **effective** cloud fractions for clouds with an optical thickness of 20, to be consistent with the assumptions made in the AMF calculations (see *Spurr, 1994*). Therefore, caution should be exercised when comparing ICFA cloud fractions with cloud fractions from other sources.

2. Summary of ICFA 2.0 validation

In this section, we will give a summary of the results of the ICFA 2.0 validation. More detailed information can be found in *Koelemeijer et al., 1997*.

2.1. Comparison with ATSR-2 data

Figure 1 shows results of a comparison of ICFA 1.5 cloud fractions (nearly identical to ICFA 2.0) with cloud fractions derived from Along Track Scanning Radiometer-2 (ATSR-2) data, acquired on 23 July 1995 over West-Europe. From the ATSR-2 reflectivity measurements, an effective cloud fraction for optically thick clouds is derived for each ATSR-2 pixel. Then the ATSR-2 cloud fractions are averaged over the GOME ground pixel. In general, reasonable correlation is found, although for orbit 1335 the ATSR-2 cloud fractions are lower than the ICFA cloud fractions, whereas for orbit 1336 the ATSR-2 cloud fractions are higher than ICFA.

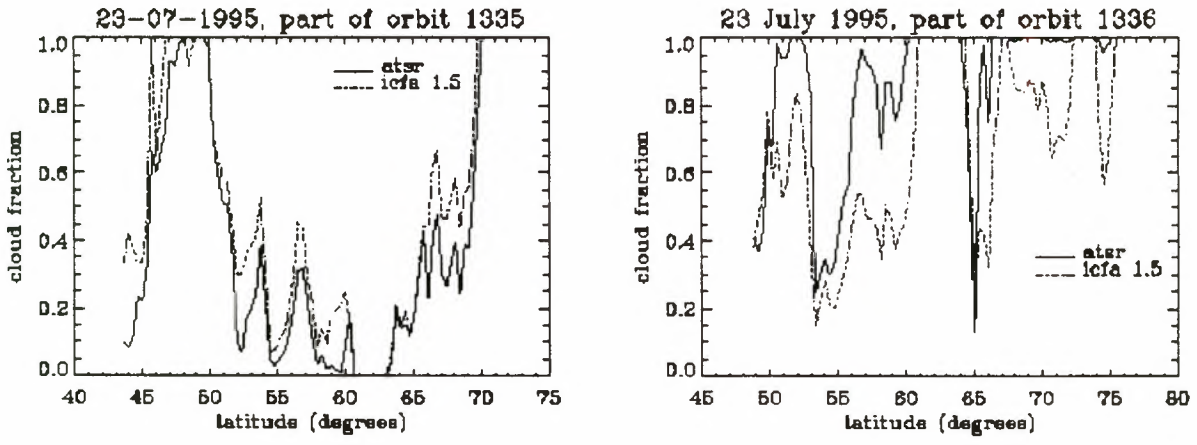

Figure 1: *Cloud fractions from ICFA version 1.5 compared with cloud fractions derived from ATSR-2 data. The data were acquired on 23 July 1995 over West-Europe.*

2.2. Comparison with ISCCP data

Also, a statistical validation approach is followed by comparing monthly averaged ICFA results (version 2.0) with monthly averaged cloud fractions from the International Satellite Cloud Climatology Project (ISCCP) (*Schiffer and Rossow, 1983; Rossow and Garder, 1993*). Figure 2 shows the monthly average ISCCP cloud fraction for July 1989 (top), and monthly average ICFA cloud fraction (below) for July 1996. The ISCCP cloud fraction is irrespective of cloud optical thickness, and is therefore in general much higher than the ICFA cloud fraction. The main global cloud structures which can easily be recognised in the ISCCP data can also (but less clear) be recognised in the ICFA data. For example, high cloud fractions occur in ISCCP and ICFA maps in the intertropical convergence zone around the Equator, and at the Southern Hemisphere off the west coast of Africa and North and South America. Over the Saharan and Middle Eastern deserts however, ICFA 2.0 cloud fractions are much too high. Also over Greenland, ICFA gives very high cloud fractions, indicating that ICFA 2.0 cannot distinguish between snow and clouds. This may also introduce errors in cloud fractions for snow-covered land areas which occur at the Northern Hemisphere during the winter.

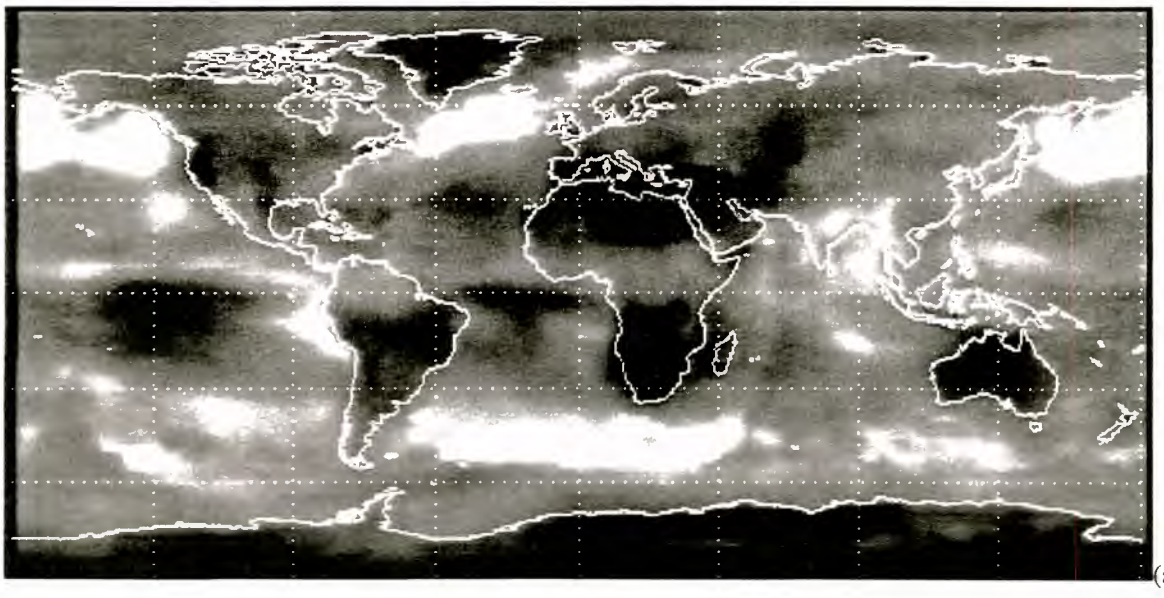

(a) ISCCP

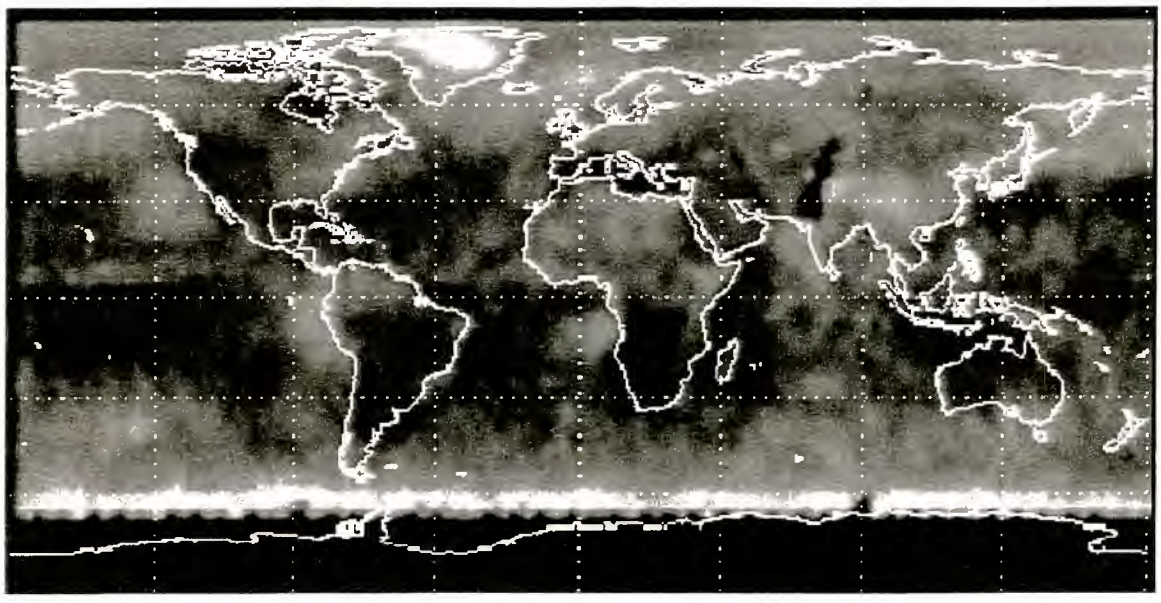

(b) ICFA

Figure 2: *Monthly average ISCCP cloud fraction for July 1989 (top), and monthly average ICFA 2.0 cloud fraction (below) for July 1996. Black: cloud fraction = 0, white: cloud fraction = 1.*

The monthly average ISCCP and ICFA 2.0 cloud fractions are averaged further by averaging over surface types. The average values are shown in Table 1.

Table 1: *Monthly average July cloud fractions from ISCCP and ICFA 2.0 for different surface types.*

Surface type	cloud fraction	
	ISCCP	ICFA
Global	0.63	0.43
Ocean	0.68	0.43
Vegetation	0.50	0.43
Desert	0.27	0.48
Snow	0.33	0.73

2.3. Conclusions ICFA 2.0 validation

In conclusion, ICFA 1.5 (nearly identical to ICFA 2.0) correlates reasonably well with cloud fractions derived from ATSR-2 data over West-Europe. In the ISCCP data, the average cloud fractions over ocean are higher than over vegetated areas. This difference, however, does not show up in the cloud fractions of ICFA 2.0. Furthermore, ICFA 2.0 gives too high cloud fractions over surfaces with a high surface albedo (desert, snow areas).

3. Comparison of ICFA 2.0 and 2.3

3.1. Analysis for 11 orbits of September 1996

In this section, we will investigate the differences in performance of ICFA between version 2.0 and 2.3. To this end, we analysed data of 11 orbits acquired during September 1996. For one orbit (orbit 7405, 19 Sept. 1996), the ICFA cloud fractions are shown along the orbit (nadir pixels only). Apparently, the ICFA 2.3 cloud fractions correlate with those of ICFA 2.0, but the ICFA 2.3 cloud fractions are much lower than those of ICFA 2.0.

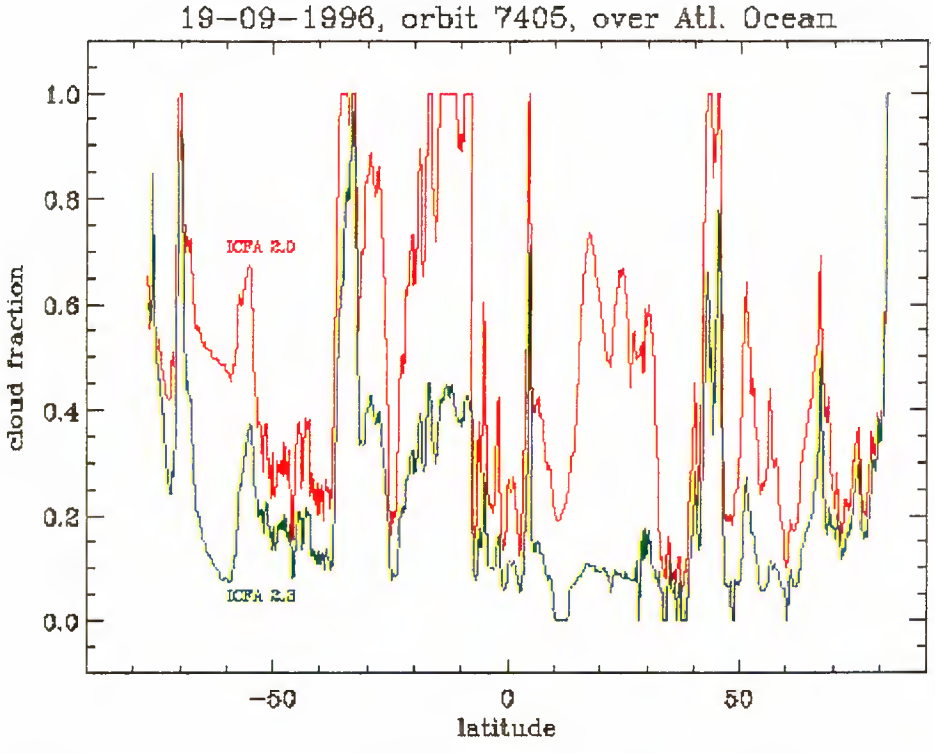

Figure 3: *ICFA cloud fractions as function of latitude (nadir pixels only). Red curve: ICFA 2.0; green curve: ICFA 2.3.*
Correlation plots of ICFA 2.0 and ICFA 2.3 over different surface types are shown in Fig. 4 (data from 11 orbits). Clearly, the decrease in cloud fraction is larger over vegetated area than over ocean, and especially cloud fractions over desert areas are much lower now. Over snow areas, the decrease in cloud fraction is sometimes large, and sometimes small. Table 2 shows the average decrease in cloud fractions between ICFA 2.0 and ICFA 2.3.

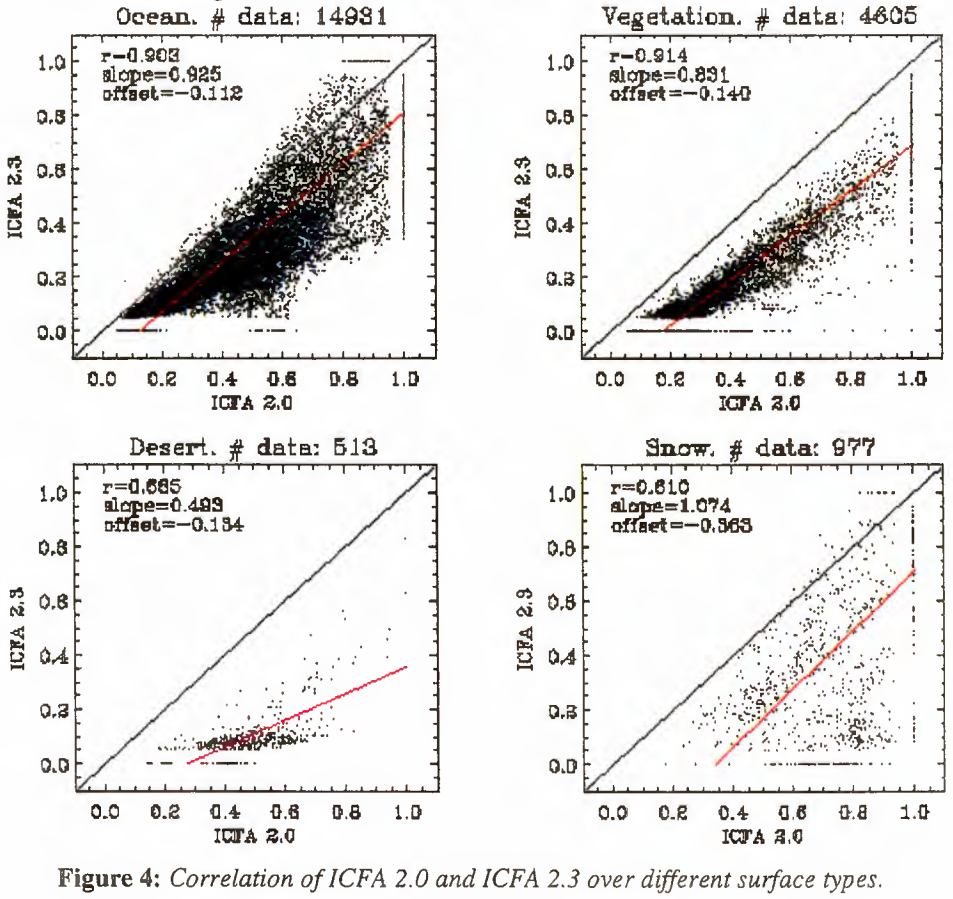

Figure 4: *Correlation of ICFA 2.0 and ICFA 2.3 over different surface types.*

Table 2: *Average cloud fractions of ICFA 2.0 and ICFA 2.3 over different surface types. Data from 11 orbits of September 1996.*

Surface type	cloud fraction		rel. diff.
	ICFA 2.0	ICFA 2.3	(2.3-2.0)/2.0
Ocean	0.486	0.337	-31 %
Vegetation	0.437	0.223	-49 %
Desert	0.484	0.105	-78 %
Snow	0.746	0.439	-41 %

3.2 Update of ICFA 2.0 validation results

The relationship between ICFA 2.0 and 2.3 presented in Table 2 has been used to make an update of the ICFA 2.0 validation results. Table 3 shows the normalised monthly average July cloud fractions from ISCCP, ICFA 2.0, and ICFA 2.3 for different surface types. The cloud fractions are **normalised by the cloud fraction over ocean**.

Table 3: *Normalised monthly average July cloud fractions from ISCCP, ICFA 2.0, and ICFA 2.3 (assuming relationship derived in Section 3.1) for different surface types.*

Surface type	ISCCP	ICFA 2.0	"ICFA 2.3"
Ocean	1	1	1
Vegetation	0.74	1.00	0.74
Desert	0.40	1.12	0.35
Snow	0.49	1.70	1.44

Apparently, the relative cloud amounts of ICFA version 2.3 over different surface types show a much better agreement with those of ISCCP. However, over snow, ICFA 2.3 cloud fractions are still too high.

4. Conclusions

The cloud fractions from ICFA version 2.3 are in general lower than those of ICFA version 2.0. The difference between ICFA 2.3 and 2.0 depends on surface type. The relative cloud amounts from ICFA 2.3 over ocean, vegetated area, and desert are similar to those of ISCCP. Therefore, we conclude that the cloud fractions of ICFA version 2.3 have improved compared to ICFA version 2.0. However, over snow covered areas, the ICFA cloud fractions are too high compared to cloud fractions over other surface types.

References

Koelemeijer, R.B.A., P. Stammes, and J.A. Konings: "Validation of GOME cloud cover fraction relevant for accurate ozone retrieval", in: *EOS/SPIE Proceedings 3220 "Satellite Remote Sensing of Clouds and the Atmosphere"*, 22-26 Sept. 1997, London, pp. 311-322.

Rossow, W. B. and L. C. Garder, "Cloud detection using satellite measurements of infrared and visible radiances for ISCCP", *J. Climate*, **6**, 2341-2369, 1993.

Schiffer, R. A. and W. B. Rossow, "The international satellite cloud climatology project ISCCP: The first project of the world climate research programme", *Bull. Amer. Meteor. Soc.*, **64**, 779-784, 1983.

Spurr, R., "GOME level 1 to 2 algorithms description", *Tech. Rep. ER-TN-DLR-GO-0025*, 32 pp., DLR, Oberpfaffenhofen, 1994.

3. Summary and Conclusions

In general, the results of the validation show the level of improvement of the new version of the GOME products correspond to the expectations.

The new products have in first place been carefully inspected to check the differences with the existing products, as reported in Chapter 1. The changes are described individually and the expected improvement quantified in a global analysis. No definite judgement of the improved quality is of course possible at this stage, but it is at least ascertained that the software implementation is correct.

Then the geophysical validity was instead assessed by mean of geophysical analyses, involving primarily the comparison with in-situ data, for both Ozone and Nitrogen Dioxide. As expected, the improvement of Ozone values is hardly detectable, while there is a notable improvement of the Nitrogen Dioxiede values, mostly due the improved climatology used in the Air Mass Factor computation.

The comparison with external data for Ozone and Nitrogen Dioxide was carried by two independent institutes (cfr Chapter 2 and Chapter 3), with difference in-situ data but similar results.

The results have been obtained on different locations with different on-ground technologies, guaranteeing the objectivity of the results.

The Ozone improvements are small, even if the retrieval is done more correctly in the physical sense. The suggested main source of errors is the climatology in use, which would be inexact in a large number of instances. Consequently the use of an algorithm less sensitive to climatology appears among the various recommendations.

The NO_2 seems more realistic in a number of cases, even though some errors are still noticeable, in particular at the extreme latitudes. The comment on the climatology is valid for the NO_2 as well, if possible with more emphasis.

In conclusion, the product can be used with the limitations outlined in Chapter 2 & 3.

The investigation of the Cloud Fitting (cfr Chapter 4) reported generally better agreement with climatological data, in our case the monthly ISCCP composites, correcting in great part the cloud fraction overestimation of the previous version. Still one can note some residual problems related to the detection of clouds over ice and snow.

Finally, the on Level 1 product, also reported in Chapter 4, it is found in general that the polarisation correction is more realistic and that it is also better collocated with the spectral data.

Overall the GOME product improvements have been confirmed with the validation exercise, and for this reason incorporated in the operational processing. No dramatic improvement has been done, but certainly correction of processing errors.

The change of processing for GOME calls for reprocessing of the historical data. This activity is certainly on the agenda, but the actual schedule will depend on the processing resources.